The Spike Response Model

Wulfram Gerstner

MNN4

September 29, 1999

ABSTRACT A description of neuronal activity on the level of ion channels, as in the Hodgkin-Huxley model, leads to a set of coupled nonlinear differential equations which are difficult to analyze. In this paper, we present a conceptual framework for a reduction of the nonlinear spike dynamics to a threshold process. Spikes occur if the membrane potential $u(t)$ reaches a threshold ϑ. The voltage response to spike input is described by the postsynaptic potential ϵ. Postsynaptic potentials of several input spikes are added linearly until u reaches ϑ. The output pulse itself and the reset/refractory period which follow the pulse are described by a function η. Since ϵ and η can be interpreted as response kernels, the resulting model is called the Spike Response Model (SRM). After a short review of the Hodgkin-Huxley model we show that (i) Hodgkin-Huxley dynamics with time-dependent input can be reproduced to a high degree of accuracy by the SRM; (ii) the simple integrate-and-fire neuron is a special case of the Spike Response Model; (iii) compartmental neurons with a passive dendritic tree and a threshold process for spike generation can be treated in SRM-framework; (iv) small nonlinearities lead to interactions between spikes to be described by higher-order kernels.

1 Introduction

The successful mathematical description of action potentials in the giant axon of the squid by Hodgkin and Huxley in 1952 has lead to a whole series of modeling papers which try to describe in detail the dynamics of various ion channels on the soma and dendrites during spike reception and spike emission. With modern computers it is now possible to numerically integrate models with 10 to 50 types of ion channel and hundreds of spatial compartments [YKA89, TWMM91, BB95] and reproduce experimental findings to a high degree of accuracy. On the other hand, it is often difficult to grasp intuitively the essential phenomena of neuronal dynamics from these models. In particular, it is out of reach to understand these models analytically. Moreover, in a network setting the question arises whether all the details described in compartmental models are necessary to understand the computation in large populations of neurons.

For an analytical understanding of networks of spiking neurons, a simplified description of neuronal dynamics is therefore desirable [AK90, Abb91]. For this reason integrate-and-fire models [Lap07, Ste67, Tuc88] have become increasingly popular for the investigation of principles of cortical dynamics and function, e.g., [MS90, AvV93, Tre93, SNS95, BH99]. The reduction of detailed neuron models to a standard integrate-and-fire unit requires simplifications in at least two respects. First, the nonlinear dynamics of *spike generation* [HH52, RE89] must be reduced to a leaky integrator with threshold firing [AK90]. Second, effects of the *spatial structure* of the neuron [Ral64, Tuc88, AFG91, BT94] must be reduced to some effective input [Abb91].

In this paper we address both issues from the systematic point of view of a response kernel expansion. It is shown that spike generation in the Hodgkin-Huxley model can be reproduced to a high degree of accuracy by a single-variable threshold model [KGvH97]. The problem of spatial structure is studied for a multi-compartmental integrate-and-fire model with a passive dendritic tree [AFG91, BT94] and active currents at the soma. In this case, the model dynamics can be solved and systematically reduced to a single-variable model with response kernels.

After the reduction of the intricate neuronal dynamics to a threshold model, it is then possible to study *analytically* the dynamics of networks of neurons. It has been shown previously that in a large network of model neurons with homogeneous couplings, the stability of coherent, incoherent, or partially coherent states can be understood in a transparent manner [AvV93, GvH93, Ger95, GvHC96, BH99]. Moreover, the collective response of a population of spiking neurons to a common *time-dependent* input can be analyzed [Ger00]. The mathematical considerations that are necessary for a reduction of the highly nonlinear Hodgkin-Huxley equations to a single-variable threshold model are therefore worth the effort.

The chapter is organized as follows. We start in section 2 with a review of the standard Hodkgin-Huxley model. The four differential equations of Hodgkin and Huxley give an accurate description of neuronal spiking in the giant axon of the squid. The drawback is that they are highly non-linear and therefore difficult to analyze mathematically. We therefore aim for a simpler phenomenological description. The method we propose is based on spike response kernels and provides a biologically transparent description of the essential effects during spiking. In the second part of section 2, we will see that the Spike Response Model (SRM), derived from the Hodgkin-Huxley model by the Spike Response Method, can reproduce up to 90 percent of the spike times of the Hodkgin-Huxley model correctly.

A short summary of the mathematics of the Spike Response Model is presented in section 3. Another well-known model of neuronal spiking is the integrate-and-fire model which is reviewed in section 4. We show that the integrate-and-fire is in fact of special case of the Spike Response Model. The mapping from the integrate-and-fire model to the Spike Response Model is discussed in some detail in sections 4.3. and 4.4. In section 5 we address the question of spatial structure. We show that in the case of a linear dendritic tree the dynamics can be well captured by spike response kernels. Finally in section 6 we discuss weakly non-linear effects. Throughout the text, the general arguments are interupted by examples intended to illustrate the main results.

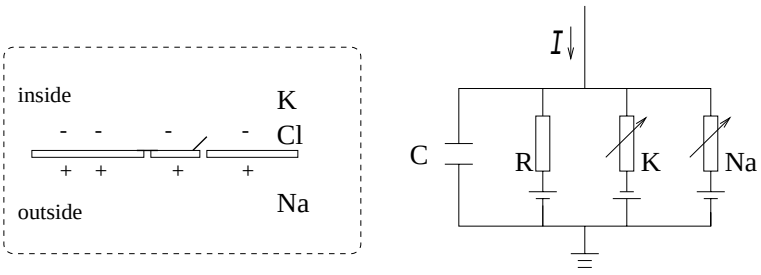

FIGURE 1. Schematic diagram for the Hodgkin-Huxley model. Taken from [Ger98].

2 Hodgkin-Huxley model

The classic description of neuronal spiking dates back to Hodgkin and Huxley [HH52] who summarized their extensive experimental studies on the giant axon of the squid with four differ ential equations. A first and fundamental equation describes the conservation of electric currents. Then there are three further differential equations which describe the dynamics of sodium and potassium ion channels. Modern models of neuronal dynamics make use of the same type of equations, but often involve many more different ion channel types. The ion channels may be located on different compartments of a spatially extended neuron model. A single neuron may then be described by hundreds of coupled non-linear differential equations. In this section we stick to the standard Hodgkin-Huxley model without spatial structure and use it as a reference model to study the dynamics of spike generation. In the first subsection we review the Hodgkin-Huxley equations. In the second subsection we reduce the nonlinear dynamics of the Hodgkin-Huxley model to a threshold model with a single variable $u(t)$. This reduction will be the basis for a discussion of the Spike Response Model in Sections 3-6.

2.1 Definition of the model

The Hodgkin-Huxley model can be understood with the help of Fig. 1. The semipermeable cell membrane separates the interior of the cell from the extracellular liquid. Due to the membrane's selective permeability and also because of active ion transport through the cell membrane, the ion concentration inside the cell is different from the one in the extracellular liquid. The difference in concentration generates an electrical potential between the interior and the exterior of the cell. The cell membrane acts like a capacitor which has been charged by a battery. If an input current $\mathcal{I}(t)$ is injected into the cell, it may add further charge on the capacitor, or leak through the channels in the cell membrane.

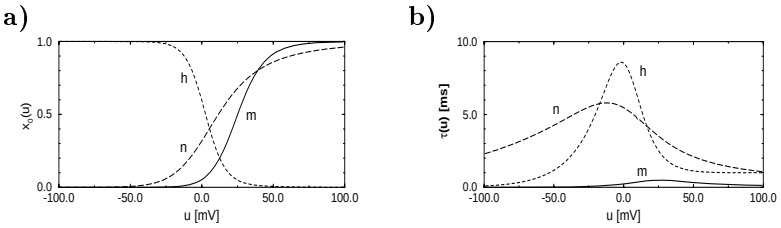

FIGURE 2. Equilibrium function (**a**) and time constant (**b**) for the three variables m, n, h in the Hodgkin-Huxley model. Taken from [Ger98].

Let us now translate the above considerations into mathematical equations. The conservation of electric charge on a piece of membrane implies that the applied current $\mathcal{I}(t)$ may be split in a capacitive current $\mathcal{I}_C$ which charges the capacitor C and further components I_k which diffuse through the ion channels. Thus

$$\mathcal{I}(t) = \mathcal{I}_C + \sum_k \mathcal{I}_k \tag{1.1}$$

where the sum runs over all ion channels. In the standard Hodgkin-Huxley model there are only three types of channel: a sodium channel with index Na, a potassium channel with index K and an unspecific leakage channel with resistance R; cf. Fig. 1. From the definition of a capacity $C = Q/u$ where Q is a charge and u the voltage across the capacitor, we find the charging current $\mathcal{I}_C = C\, du/dt$. Hence from (1.1)

$$C\frac{du}{dt} = -\sum_k I_k + \mathcal{I}(t)\,. \tag{1.2}$$

In biological terms, u is the voltage across the membrane and $\sum_k I_k$ is the sum of the ionic currents which pass through the cell membrane.

As mentioned above, the Hodgkin-Huxley describes three types of channel. All channels may be characterized by their resistance or, equivalently, by the conductance. The leakage channel is described by a voltage-independent conductance $g_L = 1/R$; the conductance of the other ion channels is voltage dependent. If the channels are fully open, they transmit currents with a maximum conductance $g_{\rm Na}$ or $g_{\rm K}$, respectively. Normally, however, the channels are partially blocked. The removal of the block is voltage dependent and is described by additional variables m, n, and h. The combined action of m and h controls the Na channels. The K gates are controlled by n. Specifically, Hodgkin and Huxley formulated the three current components as

$$\sum_k I_k = g_{\rm Na} m^3 h\,(u - V_{\rm Na}) + g_{\rm K} n^4\,(u - V_{\rm K}) + g_L\,(u - V_L). \tag{1.3}$$

The parameters $V_{\rm Na}$, $V_{\rm K}$, and V_L are called reversal potentials since the

x	u_x	g_x
Na	115mV	120mS/cm^2
K	-12mV	36mS/cm^2
L	10.6mV	0.3mS/cm^2

x	$\alpha_x(u \,/\, \mathrm{mV})$	$\beta_x(u \,/\, \mathrm{mV})$
n	$(0.1 - 0.01\,u) \,/\, [\exp(1 - 0.1\,u) - 1]$	$0.125 \exp(-u \,/\, 80)$
m	$(2.5 - 0.1\,u) \,/\, [\exp(2.5 - 0.1\,u) - 1]$	$4 \exp(-u \,/\, 18)$
h	$0.07 \exp(-u \,/\, 20)$	$1 \,/\, [\exp(3 - 0.1\,u) + 1]$

TABLE 1.1. The parameters of the Hodgkin-Huxley equations. The membrane capacity is $C = 1\mu\mathrm{F/cm}^2$.

direction of a current I_k changes when u crosses V_k. Reversal potentials and conductances are empirical parameters and summarized in table 1.

The three variables m, n, and h evolve according to the differential equations

$$\begin{aligned} \dot{m} &= \alpha_m(u)(1-m) - \beta_m(u)m \\ \dot{n} &= \alpha_n(u)(1-n) - \beta_n(u)n \\ \dot{h} &= \alpha_h(u)(1-h) - \beta_h(u)h \end{aligned} \tag{1.4}$$

with $\dot{m} = dm/dt$, and so on. The α and β, given in table 1, are empirical functions of u that have been adjusted by Hodgkin and Huxley to fit the data of the giant axon of the squid. Eqs. (1.2) - (1.4) define the Hodgkin-Huxley model.

Each of the three equations (1.4) may also be written in the form

$$\dot{x} = -\frac{1}{\tau_x(u)}[x - x_0(u)] \tag{1.5}$$

where x stands for m, n, or h. For fixed voltage u, the variable x approaches the value $x_0(u)$ with a time constant $\tau_x(u)$. The asymptotic value $x_0(u)$ and the time constant $\tau_x(u)$ are given by the transformation $x_0(u) = \alpha_x(u)/[\alpha_x(u) + \beta_x(u)]$ and $\tau_x(u) = [\alpha_x(u) + \beta_x(u)]^{-1}$. Using the parameters given by Hodgkin and Huxley [HH52], we have plotted in Fig. 2 the functions $x_0(u)$ and $\tau_x(u)$.

2.1.1 Example: Spike generation

We see from Fig. 2*a* that m_0 and n_0 increase with u whereas h_0 decreases. Thus, if some external input causes the membrane voltage to rise, the ion conductance of sodium (Na) increases due to increasing m and positive sodium ions flow into the cell. This raises the membrane potential even further. If this positive feedback is large enough, an action potential is initiated.

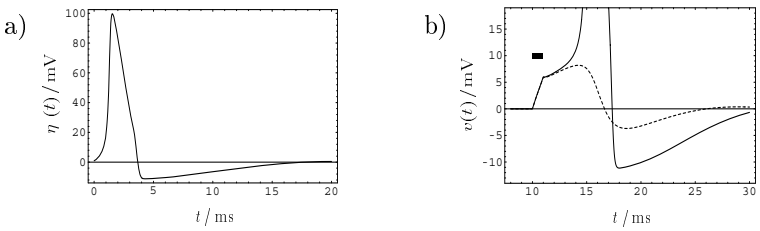

FIGURE 3. a) *Action potential.* The Hodgkin-Huxley model has been stimulated by a short, but strong, current pulse before $t = 0$. The time course of the membrane potential $u(t)$ for $t > 0$ shows the action potential (positive peak) followed by a relative refractory period where the potential is below the resting potential. The resting potential has been set to zero. In the spike response framework, the time course $u(t)$ of the action potential for $t > 0$ defines the kernel $\eta(t)$. b) *Threshold effect* in the initiation of an action potential. A current pulse of 1 ms duration has been applied at t=10 ms. For a current amplitude of 7.0 μA/cm^2, an action potential with an amplitude of about 100 mV as in *a* is initiated (solid line, the peak of the action potential is out of bounds). If the stimulating current pulse is slightly weaker (6.9 μA/cm^2) no action potential is emitted (dashed line) and the voltage v stays always below 10 mV. Note that the voltage scale in b is different from the one in a. Taken from [KGvH97].

At high values of u the sodium conductance is shut off due to the factor h. Note from Fig. 2*b* that τ_h is always larger than τ_m. Thus the variable h which closes the channels reacts more slowly to the voltage increase than the variable m which opens the channel. On the same slower time scale, the potassium (K) current sets in. Since it is a current in outward direction, it lowers the potential. The overall effect of the sodium and potassium currents is a short action potential followed by a negative overshoot.

In Fig. 3*a* we show the time course of the membrane voltage $u(t)$ during an action potential. The spike has been initiated by a short current pulse of 1 ms duration applied at $t < 0$. Note that the amplitude of the spike is about 100 mV. If the size of the stimulating current pulse is reduced below some critical value, the membrane potential returns to the rest value without a large spike-like excursion; cf. Fig. 3b. Thus we have a threshold-type behaviour.

2.1.2 Example: Constant input and mean firing rates

The Hodgkin-Huxley equations (1.2)-(1.4) may also be studied for constant input $\mathcal{I}(t) = \mathcal{I}_0$ for $t > 0$. (The input is zero for $t \leq 0$). If the value $\mathcal{I}_0$ of the stimulation is larger than a critical value I_θ, we find a regular spiking behavior. We may define a firing rate $\nu = 1/T$ where T is the interspike interval. The firing rate as a function of the constant input $\mathcal{I}_0$ is plotted in Fig. 4*b*. Spike trains with intervals $T = 1/\nu$ occur if the input current $\mathcal{I}_0$ is larger than a threshold value $\mathcal{I}_\theta \approx 6\,\mu$A/cm^2.

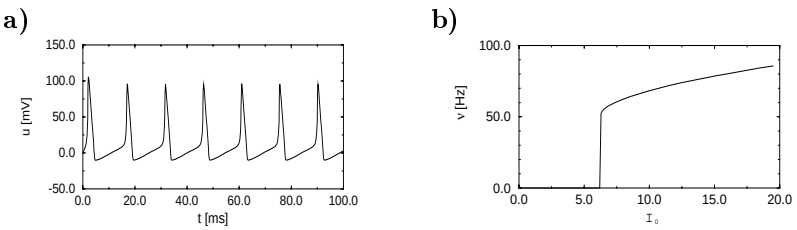

FIGURE 4. (a) *Spike train* of the Hodgkin-Huxley model for constant input current $\mathcal{I}_0$. The mean firing rate as a function of $\mathcal{I}_0$ is shown in (b).

2.1.3 Example: Step current input

In the previous example we have seen that a constant input current $\mathcal{I}_0 > I_\theta$ generates regular firing. In this paragraph we generalize this approach and study the response of the Hodgkin-Huxley model to a step current of the form

$$\mathcal{I}(t) = \mathcal{I}_1 + \Delta\mathcal{I}\,\mathcal{H}(t)\,. \tag{1.6}$$

Here $\mathcal{H}(t)$ denotes the Heaviside step function. At $t = 0$ the input changes from a constant value $\mathcal{I}_1$ to a new constant value $\mathcal{I}_2 = \mathcal{I}_1 + \Delta\mathcal{I}$; see Fig. 5*a*. We may now ask whether spiking for $t > 0$ depends only on the final value $\mathcal{I}_2$ or also on the step size $\Delta\mathcal{I}$.

The answer to this question is given by Fig. 5*b*. A large step $\Delta\mathcal{I}$ facilitates the spike initiation. Even for $\mathcal{I}_2 = 0$ a spike is possible, provided that the step size is large enough. This is an example of inhibitory rebound: A single spike is fired, if an inhibitory current $\mathcal{I}_1 < 0$ is released. The letter S in Fig. 5*b* denotes the regime where only a single spike is initiated. Repetitive firing (regime R) is possible for $\mathcal{I}_2 > 6\mu\text{A/cm}^2$, but must be triggered by sufficiently large current steps.

We may conclude from Fig. 5*b* that there is no unique current threshold for spike initiation: The trigger mechanism for action potentials depends not only on $\mathcal{I}_2$ but also on the size of the current step $\Delta\mathcal{I}$. More generally, it can be shown that the concept of a threshold itself is questionable from a mathematical point of view [RE89, KpBD95]. In a mathematical sense, the transition in Fig. 3*b*, that 'looks' like a threshold is, in fact, smooth. At a higher resolution of the input current in the regime between 6.9 and 7.0 $\mu\text{A/cm}^2$, we would find a family of response curves in between the curves shown in Fig. 3*b*. For practical purposes, however, the transition can be treated as a threshold effect as we will see below.

2.1.4 Example: Stimulation by time-dependent input

As a final example, we stimulate the Hodgkin-Huxley model by a time-dependent input current $\mathcal{I}(t)$. In the numerical implementation, the current is generated by the following procedure. Every 2 ms, a random number is drawn from a Gaussian distribution with zero mean and standard deviation

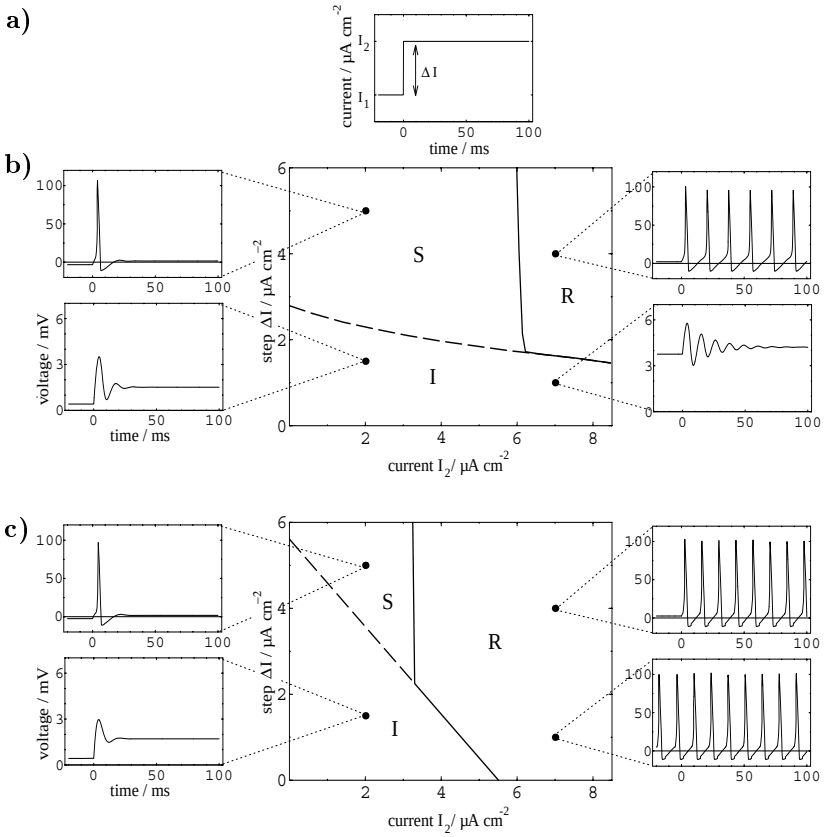

FIGURE 5. *Phase diagram* for stimulation with a step current. (a) The input current $\mathcal{I}(t)$, shown in the top graph, changes at $t = 0$ from $\mathcal{I}_1$ to $\mathcal{I}_2$. (b) Hodgkin-Huxley model and (c) Spike Response Model with optimal kernels. Three regimes denoted by S, R, and I may be distinguished. In I no action potential is initiated (inactive regime). In S, a single spike is initiated by the current step (single spike regime). In R, continuing spike trains are triggered by the current step (repetitive firing). Examples of voltage traces in the different regimes are presented in the smaller graphs to the left and right of the phase diagram in the center. Note that the Spike Response Model shows qualitatively the same behavior as the Hodgkin-Huxley model but phase boundaries are not at exactly the same location. Taken from [KGvH97].

$\sigma = 3\mu\text{A}/\text{cm}^2$. To get a continuous input current, a linear interpolation was used between the target values. The resulting time-dependent input current was then applied to the Hodgkin-Huxley model (1.2). The response to the current is the voltage trace shown in Fig. 6. Note the action potentials which occur at irregular intervals.

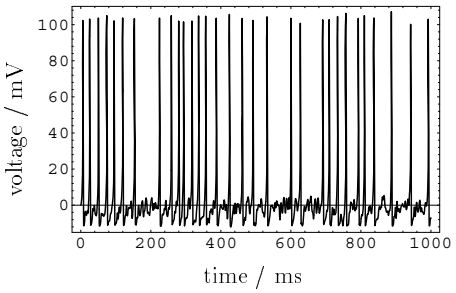

FIGURE 6. Spike train of the Hodgkin-Huxley model driven by a time dependent input current. The action potentials ocurr irregularly. The figure shows the voltage u as a function of time. Taken from [Kistler et al., 1997].

2.1.5 Extensions

Using the above equations and an appropriate set of parameters, Hodgkin and Huxley were able to describe an enormous amount of data from experiments on the giant axon of the squid. Due to its success in this special system, there have subsequently been several attempts to generalize the model in order to describe other experimental situations as well (for a review see, e.g., [JNT75, BB95]).

Whereas the model had originally been designed to describe the form and temporal change of an action potential during *axonal* transmission, a set of equations completely analogous to Eqs. (1.2) to (1.4) has been used to describe spike generation at the *soma* of the neuron [BDMK91, BD91, EWL$^+$91, RYS92, TWMM91, WBUB89, YKA89]. The main difference is that additional ion channels have to be included, in particular those that account for Ca^{2+} and the slow components of the potassium current. For each type of ion channel i, a current $I_i = g_i x_i^{n_i}(u - V_i)$ is added. Here x_i is yet another variable with dynamics (1.5). The conductance parameters g_i, the exponents n_i, the reversal potential V_i, as well as the functions $x_0(u)$ and $\tau(u)$ are adjusted to fit experimental data. Nonlinear effects on dendrites are described analogously.

2.2 Simplification of the model: Spike Response Method (1)

The system of equations proposed by Hodgkin and Huxley is rather complicated. It consists of four coupled nonlinear differential equations and as such is difficult to analyze mathematically. For this reason, several simplifications of the Hodgkin-Huxley equations have been proposed. The most common approach reduces the set of four differential equations to a system of two equations [Fit61, NAY62, Rin85, RE89, AK90]. Two important approximations are made. First, the m dynamics which has a faster time course than the other variables (see the plot for τ_m in Fig. 2*b*) is considered

to be instantaneous, so that m can be replaced by its equilibrium value $m_0(u)$. Second, the equations for n and h which have according to Fig. 2*b* roughly the same time constants are replaced by a single effective variable. Rinzel [Rin85] and Abbott and Kepler [AK90] have shown how to make such a reduction systematically. The resulting two-dimensional model is often called the Morris LeCar model or the FitzHugh-Nagumo Model. The advantage of a two-dimensional set of equations is that it allows a systematic phase plane analysis. For a review of the methods and results see the excellent article of Rinzel and Ermentrout [RE89]. For a further reduction of the two-dimensional model to an integrate-and-fire model, see the article of Abbott and Kepler [AK90].

In this subsection, we will take a somewhat different approach [KGvH97]. We would like to reduce the four Hodgkin-Huxley equations to a single variable $u(t)$. We identify u with the membrane potential of the neuron. As we have seen in Fig. 3b, the Hodgkin-Huxley model shows a sharp, threshold-like transition between an action potential (spike) for a strong stimulus and graded response (no spike) for a slightly weaker stimulus. This suggests the idea that emission of an action potential can be described by a treshold process.

In the simplified model, an action potential will be fired if the voltage $u(t)$ approaches a formal threshold ϑ from below. Let us suppose that the threshold is reached at a time $t^{(f)}$ defined by

$$u(t^{(f)}) = \vartheta \quad \text{and} \quad \frac{d}{dt} u(t^{(f)}) > 0\,. \tag{1.7}$$

We call $t^{(f)}$ the *firing time* of the neuron. If there are several neurons we add a lower index to identify the neuron so that $t_i^{(f)}$ is one of the firing times of neuron i. Let us write $\hat{t}_i := \max\{t_i^{(f)} | t_i^{(f)} < t\}$ for the *last* firing time of neuron i. In the following we only have a single neuron and we suppress the subscript i. The notation $\hat{t}$ stands for the last firing time of this neuron.

Action potentials in the Hodgkin-Huxley model have the stereotyped time course shown in Fig. 3a. Whatever the stimulating current that has triggered the spike, the form of the action potential is always roughly the same (as long as the current stays in a biologically realistic regime). This is the major observation that we will exploit in the following. Let us consider the spike triggered at time $\hat{t}$. If no further input is applied for $t > \hat{t}$, the voltage trajectory will have a pulse-like excursion before it eventually returns to the resting potential. For $t > \hat{t}$, we may therfore set $u(t) = \eta(t-\hat{t}) + u_{\rm rest}$ where η is the standard shape of the pulse and $u_{\rm rest}$ is the resting potential that the neuron assumes in the absence of any input. Since, without further input, the voltage will eventually approach the resting value, we have $\eta(t-\hat{t}) \to 0$ for $t - \hat{t} \to \infty$.

Let us now consider an additional small input current pulse $\mathcal{I}$ which is applied at $t' > \hat{t}$. Due to the input, the membrane potential will be slightly

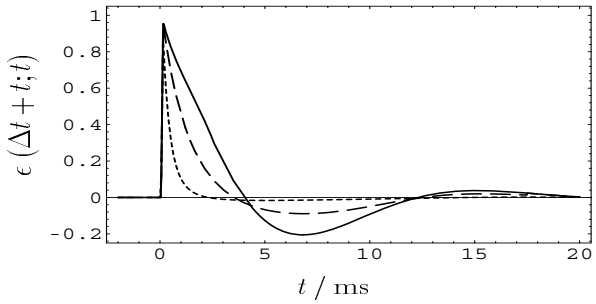

FIGURE 7. The voltage response of the Hodgkin-Huxley model to a short subthreshold current pulse defines the kernel $\tilde{\epsilon}$. The input pulse has been applied at $t = 0$. The last output spike occured at $\hat{t} = -\Delta t$. We plot the time course $\tilde{\epsilon}(\Delta t + t, t)$ (the tilde has been suppressed in the figure legend). For $\Delta t \to \infty$ we get the response shown by the solid line. For finite Δt, the duration of the response is reduced due to refractoriness (dashed line, ouput spike $\Delta t = 10.5$ ms before the input spike; dotted line $\Delta t = 6.5$ ms) taken from [Kistler et al., 1997].

perturbed from its trajectory. If the input current is sufficiently small, we may describe the perturbation by a linear impulse response function $\tilde{\epsilon}$. Since the voltage u depends on the last firing time $\hat{t}$, the response kernel $\tilde{\epsilon}$ does so as well. For an input with arbitrary time course $I(t')$ for $t' > \hat{t}$ we therefore set

$$u(t) = \eta(t - \hat{t}) + \int_0^{t-\hat{t}} \tilde{\epsilon}(t - \hat{t}, s)\, \mathcal{I}(t - s)\, ds + u_{\rm rest}\,. \tag{1.8}$$

(1.8) will be called the Spike Response Model (SRM). Note that after an appropriate shift of the voltage scale the resting potential can always be set to zero, $u_{\rm rest} = 0$.

To construct an approximative mapping between the SRM (1.8) and the Hodgkin-Huxley equations, we have to determine the following three terms (i) the kernel η which describes the response to spike emission, (ii) the kernel $\tilde{\epsilon}$ which describes the response to incoming current, and (iii) the value of the threshold ϑ in Eq. (1.7).

2.2.1 The η-kernel

In the absence of input the membrane potential u is at some resting value $u_{\rm rest}$. If we apply a strong current pulse, an action potential may be excited. The time course of the action potential determines the kernel η.

To get the kernel η we use the following procedure. We take a square current pulse of the form

$$\mathcal{I}(t) = c\,\frac{q_0}{\Delta} \quad \text{for } 0 < t < \Delta \tag{1.9}$$

and zero otherwise. q_0 is a unit charge and c a parameter chosen large enough to evoke a spike. The principle is indicated in Fig 3*b*. We consider a series of current pulses of increasing c but the same duration of $\Delta = 1$ ms. At a critical value of c the voltage response $u(t)$ shows an abrupt change from a response amplitude of about 10 mV to an amplitude of nearly 100 mV. If c is increased even further, the form of the pulse remains nearly the same. The kernel η allows us to describe the standard form of the spike and the spike afterpotential. In order to define the kernel η, we set

$$\eta(t-\hat{t}) = u(t) - u_{\rm rest} \quad \text{for} \quad t > \hat{t} \tag{1.10}$$

and $\eta(t-\hat{t}) = 0$ for $t < \hat{t}$. $u(t)$ is the voltage trajectory caused by the supra-threshold current pulse. The firing time $\hat{t}$ is defined by the moment when u crosses the formal threshold ϑ from below. The kernel $\eta(s)$ is shown in Fig. 3*a*.

2.2.2 The $\tilde{\epsilon}$-kernel

To find the kernel $\tilde{\epsilon}$ we perform a simulation with a short current as in Eq. (1.9), but with a duration $\Delta \ll 1$ ms and c sufficiently small. (Formally, we consider the limits $\Delta \to 0$ and $c \to 0$.) The voltage response of the Hodgkin-Huxley model to this sub-threshold current pulse defines the kernel $\tilde{\epsilon}$,

$$\tilde{\epsilon}(\infty, t) = \frac{1}{c}\left[u(t) - u_{\rm rest}\right] . \tag{1.11}$$

$t > 0$ is the time since the initiation of the pulse. The first argument of $\tilde{\epsilon}$ has been set to infinity in order to indicate that the neuron did not fire an action potential in the recent past.

In order to calculate ϵ for finite $t - \hat{t}$, we use a first strong pulse to initiate a spike at a time $\hat{t} < 0$ and then apply a second weak pulse with amplitude c at $t = 0$. The result is a membrane potential with time course $u(t)$. Without the second pulse the time course of the potential would be $u_0(t) = \eta(t-\hat{t}) + u_{\rm rest}$ for $t > \hat{t}$. The response to the second pulse is $u(t) - u_0(t)$, hence

$$\tilde{\epsilon}(t-\hat{t}, t) = \frac{1}{c}\left[u(t) - \eta(t-\hat{t}) - u_{\rm rest}\right] . \tag{1.12}$$

for $t > 0$. We repeat the above procedure for various spike times $\hat{t}$.

The result is shown in Fig. 7. Since the input current pulse delivers a unit charge during a very short amount of time $\Delta < 0.1$ ms, the $\tilde{\epsilon}$-kernel jumps almost instantaneously at time $t = 0$ to a value of 1 mV. Afterwards it decays, with a slight oscillation, back to zero. The decay is faster if there has been a spike in the recent past. This is easy to understand intuitively. During and immediately after an action potential many ion channels are open. The resistance of the cell membrane is therefore reduced and the effective membrane time constant is shorter.

2.2.3 The threshold ϑ

The third term to be determined is the threshold ϑ. Even though Fig. 3*b* suggests, that the Hodgkin-Huxley equations exhibit some type of threshold behavior, the threshold is not well-defined [RE89, KpBD95] and it is fairly difficult to estimate a voltage threshold directly from a single series of simulations. We therefore take the threshold as a free parameter which will be adjusted by a procedure discussed below.

2.2.4 Example: Stimulation by time-dependent input

To test the quality of the SRM approximation we compare the performance of the Spike Response Model (1.8) with that of the full Hodgkin-Huxley model (1.2) - (1.4). We study the case of a time-dependent input current $\mathcal{I}(t)$. The input is generated by the procedure discussed in section 2.1.4. The same current is applied to both the Hodgkin-Huxley and the Spike Response model. In Fig. 8 the voltage trace of the Hodgkin-Huxley model is compared to that of the Spike Response Model with the kernels η and $\tilde{\epsilon}$ derived above. We see that the approximation is excellent both in the absence of spikes and during spiking. As an aside we note that it is indeed important to include the dependence of the kernel $\tilde{\epsilon}$ upon the last output spike time $\hat{t}$. If we neglected that dependence and used $\tilde{\epsilon}(\infty, s)$ instead of $\tilde{\epsilon}(t - \hat{t}, s)$, then the approximation during and immediately after a spike would be significantly worse; see the dotted line, referred to as SRM_0, in the lower right graph of Fig. 8.

We have used the above scenario with time-dependent input current to optimize the threshold ϑ by the following procedure. The same input was applied to the Hodgkin-Huxley model and the Spike Response Model (1.8) with kernels derived by the procedure described above. The threshold has been adjusted so that the total number of spikes was about the same in the two models; see [KGvH97] for details.

To check whether both models generated spikes at the same time, we compared the firing times of the two models. About 90 per cent of the spikes of the Spike Response Model occurred within ± 2 ms of the action potentials of the Hodgkin-Huxley model [KGvH97]. Thus the Spike Response Model (1.8) reproduces the firing times and the voltage of the Hodgkin-Huxley model to a high degree of accuracy.

2.2.5 Example: Constant input and mean firing rates

We study the response of the Spike Response Model to constant stimulation using the kernels derived by the procedure described above. The result is shown in Fig. 9. As mentioned above, we take the threshold ϑ as a free parameter. If ϑ is optimized for stationary input, the frequency plots of the Hodgkin-Huxley model and the Spike Response Model are rather similar. On the other hand, if we took the value of the threshold that was found for

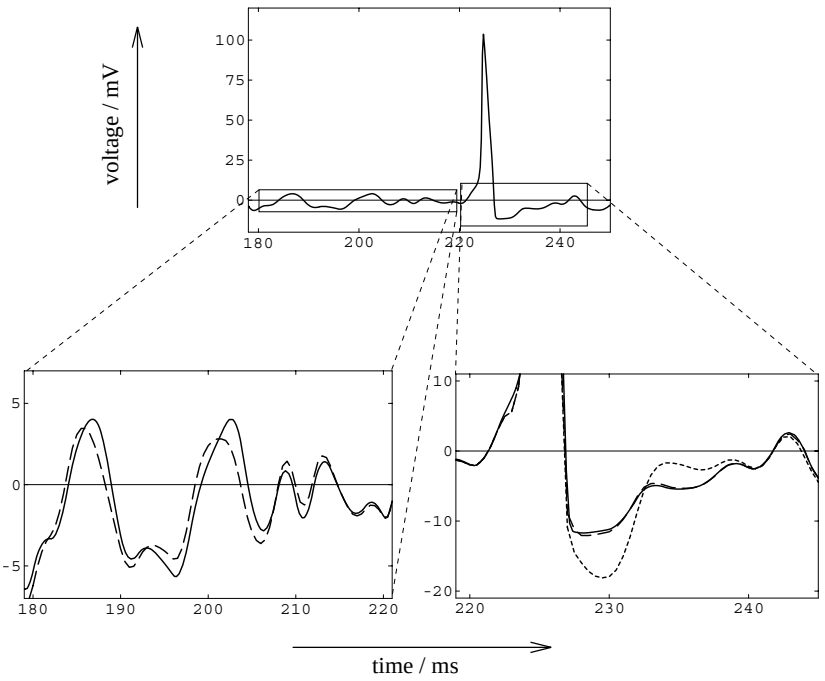

FIGURE 8. A segment of the spike train of Fig. 6. The inset in the lower left corner shows the voltage of the Hodgkin-Huxley model (solid) together with the approximation of the Spike Response Model defined by (1.8) (dashed line) during a period where no spike occurs. The approximation is excellent. The inset on the lower right shows the situation during and after a spike. Again the approximation by the dashed line is excellent. For comparison, we also show the approximation by the SRM_0 model which is significantly worse (dotted line). Taken from [KGvH97].

time-dependent input, the current threshold for the Spike Response Model would be quite different as shown by the dashed line in Fig. 9.

2.2.6 Example: Step current input

Finally, we test the Spike Response Model for the case of step current input. For ϑ we take the value found for the scenario with time-dependent input. The result is shown in Fig. 5*c*. The Spike Response Model shows the same three regimes as the Hodgkin-Huxley model. In particular, the effect of inhibitory rebound is present in the Spike Response Model. The location of the phase boundaries depends on the choice of ϑ and would move if we changed ϑ.

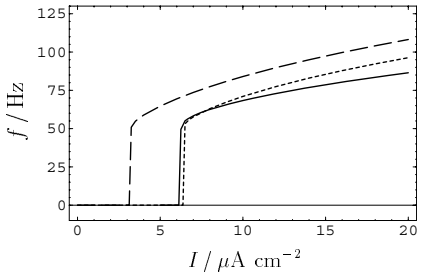

FIGURE 9. The firing rate of the Hodgkin-Huxley model (solid line) is compared to that of the Spike Response Model. Two cases are shown. If the threshold ϑ is optimized for the constant-input scenario, we get the dotted line. If we take the same value of ϑ as in the dynamic-input scenario of the previous figure, we find the dashed line. Input current has a constant value $\mathcal{I}$. Taken from [KGvH97].

2.2.7 Example: Spike input

In the Hodgkin-Huxley model (1.2), input is formulated as an explicit driving current $\mathcal{I}(t)$. In networks of neurons, input typically consists of the spikes of other, presynaptic, neurons. Let us, for the sake of simplicity, assume that a spike of a presynaptic neuron j which was emitted at time $t_j^{(f)}$ generates for $t > t_j^{(f)}$ a current input $\mathcal{I}(t) = \alpha(t - t_j^{(f)})$ to a postsynaptic neuron i. Here α is some arbitrary function which describes the time course of the postsynaptic *current*. The voltage of the postsynaptic neuron i changes, according to (1.8) by an amount $\Delta u_i(t) = \int_0^{t-\hat{t}_i} \tilde{\epsilon}(t-\hat{t}_i, s)\, \alpha(t - t_j^{(f)} - s)\, ds$ where $\hat{t}_i$ is the last output spike of neuron i. For reasons of causality, the voltage response Δu vanishes for $t < t_j^{(f)}$. For $t > t_j^{(f)}$ we define (note that there is no tilde on the left-hand side)

$$\begin{aligned} \epsilon(t-\hat{t}_i, t - t_j^{(f)}) : &= \Delta u_i(t) \\ &= \int_0^{t-\hat{t}_i} \tilde{\epsilon}(t-\hat{t}_i, s)\, \alpha(t - t_j^{(f)} - s)\, ds \end{aligned} \quad (1.13)$$

What is the meaning of the definition (1.13)? Let us assume that the last output spike of the postsynaptic neuron was a long time back in the past. The voltage response $\Delta u_i(t) = \epsilon(\infty, t - t_j^{(f)})$ is the postsynaptic potential of neuron i caused by the firing of the presynaptic neuron j. The time course of the postsynaptic potential can be measured in experiments and has a clear biological interpretation. For excitatory synapses the response of the postsynaptic neuron is positive and called an excitatiory postsynaptic potential (EPSP). For inhibitory synapses it is negative (IPSP). The function (1.13) will play a major role in the formal definition of the Spike Response Model in the following section.

3 Spike Response Model (SRM)

In this section we collect the results of the previous discussion of the Hodgkin-Huxley model. We start with a formal presentation of the Spike Response Model (SRM) in equation (1.14) and (1.15). We then try to give each of the terms in (1.15) a biological meaning. To do this we make heavily use of the intuitions and results developed during the discussion of the Hodgkin-Huxley model. Finally, we present some examples and simplifications of the SRM which prepare the transition to a discussion of the integrate-and-fire model in section 4.

3.1 Definition of the SRM

In the framework of the spike response model [KGvH97, GvH92, GvH93, Ger95, GvHC96, Ger98, Ger00, Maa96, Maa98, Cho98], the state of a neuron i is described by a single variable u_i. Neuron i fires, if u_i approaches a threshold ϑ from below. The moment of threshold crossing defines the firing time $t_i^{(f)}$,

$$u_i(t) = \vartheta \quad \textbf{and} \quad \frac{d}{dt} u_i(t) > 0 \quad \Longrightarrow t = t_i^{(f)} \tag{1.14}$$

In the absence of any spikes, the variable u_i would have a value of 0. Each incoming spike will perturb u_i and it takes some time before u_i return to zero. The function ϵ describes the time course of the response to an incoming spike. If, after the summation of the effects of several incoming spikes, u reaches the threshold ϑ an output spike is triggered. The form of the action potential followed by a return to a low value after the pulse is described by a function η. Let us suppose neuron i has fired its last spike at time $\hat{t}_i$. After firing the temporal evolution of u is given by

$$\begin{aligned} u_i(t) &= \eta_i(t-\hat{t}_i) + \sum_{j\in\Gamma_i} w_{ij} \sum_{t_j^{(f)}\in\mathcal{F}_j} \epsilon_{ij}(t-\hat{t}_i, t-t_j^{(f)}) \\ &\quad + \int_0^\infty \tilde{\epsilon}(t-\hat{t}_i, s)\, \mathcal{I}^{\text{ext}}(t-s)\, ds \end{aligned} \tag{1.15}$$

where $\hat{t}_i$ is the last spike of neuron i, $t_j^{(f)}$ are spikes of presynaptic neurons j and w_{ij} is the synaptic efficacy. The last term accounts for an external driving current $\mathcal{I}^{\text{ext}}$. The sum runs over all presynaptic neurons $j \in \Gamma_i$ where

$$\Gamma_i = \{j \,|\, j \text{ presynaptic to } i\} \tag{1.16}$$

and $\mathcal{F}_j$ is the set of all firing times $t_j^{(f)} < t$ of neuron j.

So far Eqs. (1.14) and (1.15) define a formal model. Can we give a biological interpretation of the terms? Let us identify the variable u_i with the

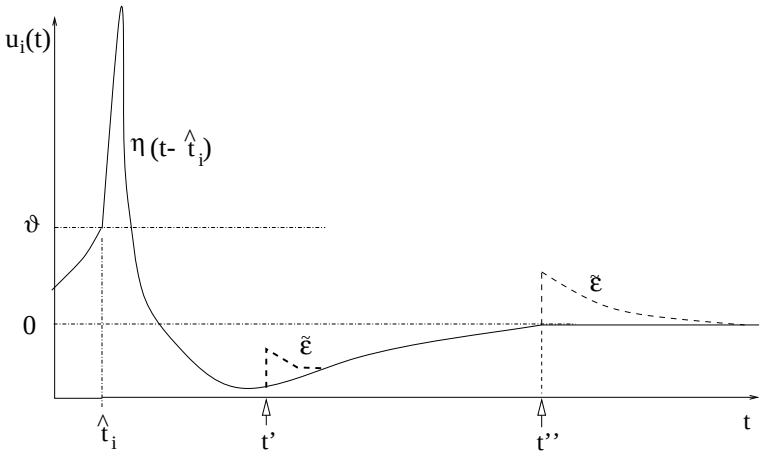

FIGURE 10. Schematic interpretation of the Spike Response Model. The figure shows the time course of the membrane potential of neuron i as a function of time t. A spike of neuron i has been initiated at $\hat{t}_i$. The kernel $\eta(t-\hat{t}_i)$ for $t > \hat{t}_i$ describes the form of the action potential (positive pulse) and the (negative) spike afterpotential that follows the pulse (solid line). If an input current pulse is applied at a time t'' a long time after the firing at $\hat{t}_i$, it evokes a standard response described by the function $\tilde{\epsilon}(\infty, t-t'')$ and indicated by the dashed line starting at t'' (arrow). An input current pulse at t' which arrives shortly after the postsynaptic spike at $\hat{t}_i$ evokes, due to refractoriness of the neuron, a response of significantly shorter duration. Its time course is described by the response kernel $\tilde{\epsilon}(t-\hat{t}_i, t-t')$; see the dashed line after t'.

membrane potential of neuron i. The functions η_i and ϵ_{ij} are *response kernels* which describe the effect of spike emission and spike reception on the variable u_i. This interpretation has motivated the term 'Spike Response Model' (SRM). Let us discuss the meaning of the response kernels; see Fig. 10.

As we have seen in section 2, the kernel η_i describes the standard form of an action potential of neuron i including the negative overshoot which typically follows a spike. Graphically speaking, a contribution η_i is 'pasted in' each time the membrane potential reaches the threshold ϑ; Fig. 10. Since the form of the spike is always the same, the exact time course of the action potential carries no information. What matters is whether there is the event 'spike' or not. The event is fully characterized by the firing time $t_i^{(f)}$. In a simplified model, the *form* of the action potential may therefore be neglected as long as we keep track of the firing times $t_i^{(f)}$. The kernel η_i describes then simply the 'reset' of the potential to a lower value after the spike at $\hat{t}_i$. This idea will be exploited later on in section 4 in the context of the intergrate-and-fire model.

The kernel $\tilde{\epsilon}(t-\hat{t}_i, s)$ is the linear response of the membrane potential

to an input current. We have already seen in Section 2 that the response depends, in general, on the time that has passed since the last output spike at $\hat{t}_i$. Immediately after $\hat{t}_i$ many ion channels are open. The resistance of the membrane is reduced and the voltage response to an input current pulse of unit amplitude is therefore reduced compared to the response of a inactive neuron. A reduced response is one of the signatures of neuronal refractoriness. Formally, this form of refractory effect is included by making the kernel $\tilde{\epsilon}$ depend, in its first argument, on the time difference $t - \hat{t}_i$. In Fig. 10 we compare the effect of an input current pulse at t' shortly after $\hat{t}_i$ to that of a pulse at t'' some time later. The response to the first input pulse is shorter and less pronounced than that to the second one.

The kernel $\epsilon_{ij}(t - \hat{t}_i, s)$ as a function of $s = t - t_j^{(f)}$ can be interpreted as the time course of a postsynaptic potential evoked by the firing of a presynaptic neuron j at time $t_j^{(f)}$. If the synapse from j to i is excitatory, ϵ_{ij} is called the excitatory postsynaptic potential (EPSP). If it is inhibitory, it is called the inhibitory postsynaptic potential (IPSP). Similarly as for the kernel $\tilde{\epsilon}$, the exact shape of the postsynaptic potential depends on the time $t - \hat{t}_i$ that has passed since the last spike of the postsynaptic neuron i. In particular, if neuron i has been active immediately before presynaptic spike arrival, the postsynaptic neuron is in a state of refractoriness. In this case, the response to an input spike is smaller than that of an 'unprimed' neuron. The first argument of $\epsilon_{ij}(t - \hat{t}_i, s)$ accounts for the dependence upon the last firing time of the postsynaptic neuron.

In order to simplify the notation later on, it is convenient to introduce the *total postsynaptic potential*

$$h_{\rm PSP}(t|\hat{t}_i) = \sum_{j\in\Gamma_i} w_{ij} \sum_{t_j^{(f)}\in\mathcal{F}_j} \epsilon_{ij}(t-\hat{t}_i, t-t_j^{(f)}) + \int_0^\infty \tilde{\epsilon}(t-\hat{t}_i, s)\, \mathcal{I}_i^{\rm ext}(t-s)\, ds\,. \tag{1.17}$$

Eq. (1.15) can then be written in the form

$$u_i(t) = \eta_i(t - \hat{t}_i) + h_{\rm PSP}(t|\hat{t}_i)\,. \tag{1.18}$$

3.1.1 Example: Refractoriness

Refractoriness may be described qualitatively by the observation that immediately after a first action potential it is much more difficult to excite a second spike. In our description two factors contribute to refractoriness; see Fig. 10. Firstly η contributes because, during the spike, the voltage is above threshold. Thus it is excluded that the membrane potential is crossed from below so that emission of another spike is by definition impossible. Moreover, after the spike the membrane potential passes through a regime of hyperpolarization (negative overshoot) where it is *below* the resting potential. During this phase, more stimulation than usual is needed to drive the membrane potential above threshold.

Secondly, ϵ and $\tilde{\epsilon}$ contribute because, immediately after an action potential, the response to incoming spikes is shorter and, possibly, of reduced amplitude. Thus more input spikes are needed to evoke the same depolarization of the membrane potential as in an 'unprimed' neuron. The first argument of the ϵ function (or $\tilde{\epsilon}$ function) allows us to incorporate this effect. If $t_j^{(f)} - \hat{t}_i \to \infty$, then the response of neuron i to a presynaptic spike of neuron j is the standard EPSP. If $t_j^{(f)}$ is close to $\hat{t}_i$, then the postsynaptic potential $\epsilon(t - \hat{t}_i, t - t_j^{(f)})$ has a different time course.

3.1.2 Example: Experimental results

In recent experiments, Stevens and Zador [SZ98] have stimulated a cortical neuron with time-dependent current and measured the response of the membrane potential during repetitive firing. In order to fit their measurements to integrate-and-fire type dynamics, they found that it was important to work with a time-varying time 'constant' $\tau(t' - \hat{t})$.

Given that the last output spike was at $\hat{t} < 0$, the response to input at $t = 0$ is (for $t > 0$) apprixmated by

$$\tilde{\epsilon}(t - \hat{t}, t) = a_0 \exp\left\{ - \int_0^t \frac{dt'}{\tau(t' - \hat{t})} \right\} \tag{1.19}$$

where a_0 is a parameter and $\tau(t' - \hat{t})$ is the instantaneous membrane time constant. Immediately after the output spike at $\hat{t}$ the membrane time constant is only about 2 ms; for $t' - \hat{t} \to \infty$ the membrane time constant increases and approaches the standard value $\tau_m \approx 10 - 15\,\mathrm{ms}$.

3.1.3 Example: SRM_0

A simpler version of the spike response model can be constructed, if we neglect the dependence of ϵ upon the first argument. We simply set

$$\begin{aligned} \epsilon_0(s) &= \epsilon_{ij}(\infty, s) \\ \tilde{\epsilon}_0(s) &= \tilde{\epsilon}_{ij}(\infty, s) \end{aligned}$$

and use (1.15) in the form

$$u_i(t) = \eta_i(t - \hat{t}_i) + \sum_{j \in \Gamma_i} w_{ij} \sum_{t_j^{(f)} \in \mathcal{F}_j} \epsilon_0(t - t_j^{(f)}) + \int_0^\infty \tilde{\epsilon}_0(s)\, \mathcal{I}^{\mathrm{ext}}(t - s)\, ds \tag{1.20}$$

Thus each presynaptic spike evokes a postsynaptic potential with the same time course, independent of the index j of the presynaptic neuron and independent of the last firing time $\hat{t}_i$ of the postsynaptic neuron. Only the amplitude of the response is scaled with the synaptic efficact w_{ij}. This simple version of the Spike Response Model has been termed SRM_0 [Ger00] and has been used for the analysis of computation with spiking neurons [Maa96, Maa98] and for that of network synchronization [GvHC96].

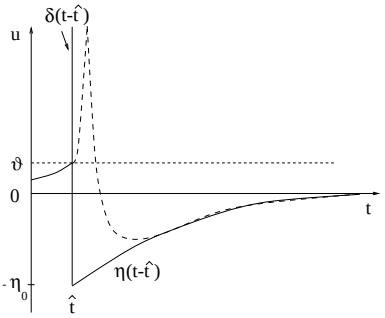

FIGURE 11. In formal models of spiking neurons, the shape of an action potential (dashed line) is replaced by a δ pulse (thick vertical line). The negative overshoot (spike after potential) after the pulse is included in the kernel $\eta(t-\hat{t})$ (thick line). The pulse is triggered by the treshold crossing at $\hat{t}$.

3.1.4 Example: From action potentials to formal events

The shape of an action potential is described by the function $\eta(t-\hat{t})$. Since it has a stereotyped time course, the form of the action potential does not transmit any information. What counts is the event 'spike' as such. In formal model, the form of the pulse is therefore often replaced by a δ function. The negative overshoot after the spike is modelled as a reset to a lower value. One of several possible descriptions is

$$\eta(t-\hat{t}) = \delta(t-\hat{t}) - \eta_0 \exp\left(-\frac{t-\hat{t}}{\tau}\right) \tag{1.21}$$

with a parameter $\eta_0 > 0$. The negative overshoot (second term on the right-hand-side of (1.21)) decays back to zero with a time constant τ. The simpification from a nicely shaped action potential to a formal η-function is illustrated in Fig. 11.

3.1.5 Example: Graphical construction of firing times

Let us now summarize the considerations of the two preceding examples and procede to a graphical illustration of the model; cf. Fig. 12. The neuron under consideration receives input from several presynaptic cells. Each input spike evokes a postsynaptic potential of some standard form $\epsilon_0(s)$. We assume excitatory synapses, so that ϵ is positive. The excitatory postsynaptic potentials are summed until the firing threshold ϑ is reached. Each output spike is approximated by a δ pulse, followed by a reset as in (1.21). Then the summation of inputs restarts.

3.1.6 Example: Coherent versus incoherent input

What can we do with the simplified neuron model defined by (1.20) and (1.21)? The Spike Response Model can provide an intuitive understanding

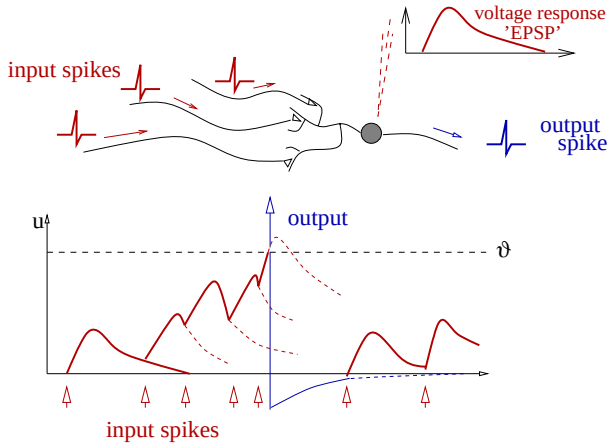

FIGURE 12. Spike Response Model SRM_0. Each input pulse causes an excitatory postsynaptic potential (EPSP) $\epsilon(s)$. All EPSPs are added. If the threshold is reached the voltage is reset. The reset corresponds to adding a negative kernel $\eta(s)$.

of questions of neuronal coding and signal transmission. For example, we may easily understand why coherent input is more efficient than incoherent input in driving a postsynaptic neuron.

To illustrate this point, let us consider an ϵ kernel of the form

$$\epsilon_0(s) = J \frac{s}{\tau} \exp(-\frac{s}{\tau}) \quad \text{for} \quad s > 0 \tag{1.22}$$

and zero otherwise. We set $J = 1$ mV and τ =10 ms. The function (1.22) has a maximum value of J/e at $s = \tau$. The integral over s is normalized to $J\tau$.

Let us consider a neuron i which receives input from 100 presynaptic neurons j. Each presynaptic neuron fires at a rate of 10 Hz. All synapses have the same efficacy $w_0 = 1$. Let us first study the case of asynchronous input. Different neurons fire at different times so that, on average, spikes arrive at intervals of $\Delta t = 1\ ms$. Each spike evokes a postsynaptic potential defined by (1.22). The total membrane potential of neuron i is

$$\begin{aligned} u_i(t) &= \eta(t - \hat{t}_i) + \sum_j \sum_{t_j^{(f)}} w_0\, \epsilon_0(t - t_j^{(f)}) \\ &\approx \eta(t - \hat{t}_i) + w_0 \sum_{n=0}^{\infty} \epsilon_0(t - n\,\Delta t) \end{aligned} \tag{1.23}$$

If neuron i has been quiescent in the recent past ($t - \hat{t}_i \to \infty$), then the first term on the right-hand side of (1.23) can be neglected. The second

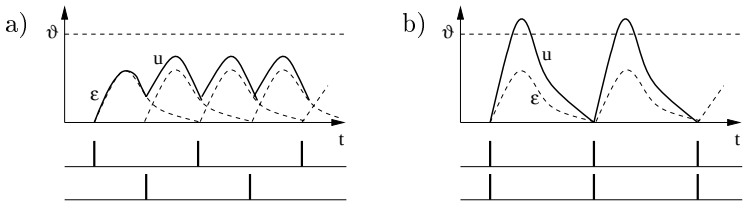

FIGURE 13. Potential u of a postsynaptic neuron which receives input from two groups of presynaptic neurons. a) Spike trains of the two groups are phase shifted with respect to each other. The total potential u does not reach the threshold. There are no output spikes. b) Spikes from two presynaptic groups arrive synchronously. The summed EPSPs reach the threshold ϑ and cause the generation of an output spike.

term can be appoximated by an integral over s, hence

$$u_i(t) \approx \frac{w_0}{\Delta t} \int_0^\infty \epsilon_0(s)\, ds = \frac{w_0\, J\, \tau}{\Delta t} = 10\ mV\,. \tag{1.24}$$

If the firing threshold of the neuron is at $\vartheta = 20$ mV the neuron stays quiescient.

Now let us consider the same numer of inputs, but fired coherently at $t_j^{(f)} = 0, 100, 200, \ldots$ ms. Thus each presynaptic neuron fires as before at 10 Hz but all presynaptic neurons emit their spikes synchronosly. Let us study what happens after the first volley of spikes has arrived at $t = 0$. The membrane potential of the postsynaptic neuron is

$$u_i(t) = \eta(t - \hat{t}_i) + N\, w_0\, \epsilon_0(t) \tag{1.25}$$

where $N = 100$ is the number of presynaptic neurons. The maximum of (1.25) occurs at $t = \tau = 10$ ms and has a value of $w_0 NJ/e \approx 37$ mV which is above threshold. Thus the postsynaptic neuron fires before $t = 10$ ms. We conclude that the same numer of input spikes can have different effects depending on their level of coherence.

In Fig. 13 we illustrate this effect for a simplified scenarios of two groups of presynaptic neurons. Neurons within each group fire synchronously. In a there is a phase shift between the spikes of the two groups, whereas in b the two groups are synchronous.

3.1.7 Example: Sliding threshold interpretation

The simplified model SRM_0 defined in (1.20) with the η kernel defined in (1.21) allows us to give a reinterpretation of refractoriness as an *increase* of the firing threshold. To see how this works, let us introduce the *input potential*

$$h_i(t) = \sum_{j \in \Gamma_i} w_{ij} \sum_{t_j^{(f)} \in \mathcal{F}_j} \epsilon_0(t - t_j^{(f)}) + \int_0^\infty \tilde{\epsilon}_0(s)\, \mathcal{I}^{\mathrm{ext}}(t - s)\, ds\,. \tag{1.26}$$

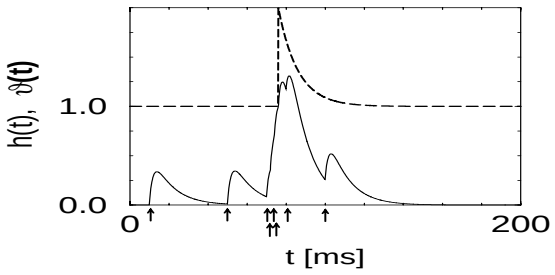

FIGURE 14. *Sliding threshold interpretation.* The input potential $h(t)$ (solid line) is generated by the superposition of the EPSPs (solid line) caused by presynaptic spikes. Each spike arrival is denoted by an arrow. An output spike occurs, if $h(t)$ hits the dynamic threshold $\vartheta(t)$ (dashed line). At the moment of spiking the value of the treshold is increased by one. After the spike, the threshold decays exponentially back to its resting value $\vartheta = 1$.

We emphasize that h_i depends on the input only. In particular, there is no dependence upon $\hat{t}_i$. With the above definition of h_i, Eq. (1.20) is simply $u_i(t) = \eta_0(t - \hat{t}_i) + h_i(t)$. The next spike occurs if $u_i(t) = \vartheta$ or

$$h_i(t) = \vartheta - \eta_0(t - \hat{t}_i)\,. \tag{1.27}$$

We may consider $\vartheta - \eta_0(t - \hat{t}_i)$ as a dynamic threshold which is *increased* after each firing. (1.27) has a simple interpretation: The next firing occurs if the input potential $h_i(t)$ reaches the dynamic threshold $\vartheta - \eta_0(t - \hat{t}_i)$ [MO74]. See Fig. 14 for an illustration.

3.2 Background

In contrast to the standard integrate-and-fire model which is usually stated in terms of differential equations, Eq. (1.15) is based on an 'integral' representation with response kernels. Eq. (1.15) is linear in the spikes and can be considered a starting point of a systematic expansion [Ger95, KGvH97]. As we will see later in section 6, nonlinear effects between pairs of spikes can be included by second-order kernels of the form $\epsilon_{ijk}(t - \hat{t}_i, t - t_j^{(f)}, t - t_k^{(f)})$. Higher order nonlinearities are treated similarly. Effects of earlier spikes of postsynaptic neurons can be treated by kernels $\eta_i(t - \hat{t}_i, t - t_i^{(2)})$, $\eta_i(t - \hat{t}_i, \ldots, t - t_i^{(k)})$ where $\hat{t}_i = t_i^{(1)}$ is the last spike of neuron i and $t_i^{(k)}$ is the kth spike counting backward in time.

The approach by spike response kernels provides a link between simplified neuron models of the form (1.15) and multi-compartmental models [YKA89, TWMM91, BB95] and presents an alternative to earlier approaches towards a reduction of Hodgkin-Huxley equations [AK90, Rin85, Fit61, KAM92].

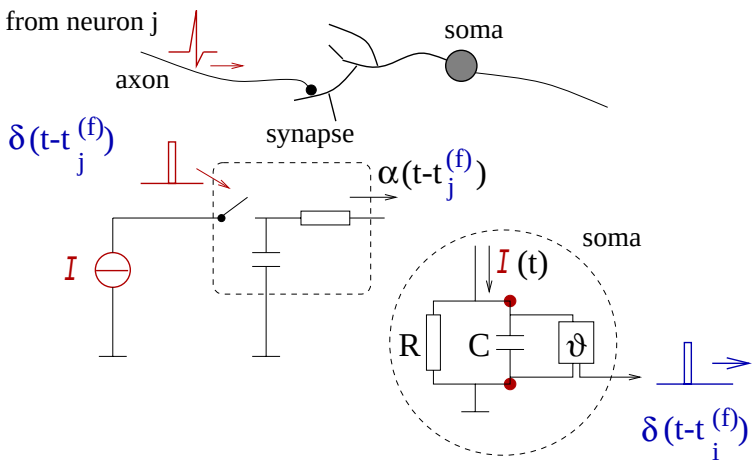

FIGURE 15. Schematic diagram of the integrate-and-fire model. The basic circuit is the module inside the dashed circle on the right-hand side. A current $\mathcal{I}(t)$ charges the RC circuit. The voltage $u(t)$ across the capacitance (points) is compared to a threshold ϑ. If $u(t) = \vartheta$ at time $t_i^{(f)}$ an output pulse $\delta(t - t_i^{(f)})$ is generated. Left part: A presynaptic spike $\delta(t - t_j^{(f)})$ is low-pass filtered at the synapse and generates an input current pulse $\alpha(t - t_j^{(f)})$.

The remainder of the chapter is organized as follows. In the following section, the integrate-and-fire neuron without spatial structure (point neuron) is reviewed. It is shown that integration of the model leads to (1.15) or (1.20). Thus, the intergrate-and-fire model is a special case of the Spike Response Model. In section 5, a spatially extended version of the integrate-and-fire model with linear dendritic tree is considered. It is shown that integration of the model leads again back to (1.15). In section 6 the problem of nonlinearities during synaptic and dendritic transmission are discussed.

4 Integrate-and-fire model

We start in the first subsection with a review of the integrate-and-fire neuron. In the following subsections we will show that the integrate-and-fire neuron is a special case of the Spike Respone Model defined in the previous section.

4.1 Definition of the basic model

The basic circuit of an integrate-and-fire model consists of a capacitor C in parallel with a resistor R driven by a current $\mathcal{I}(t)$; see Fig. 15, dashed circle. The driving current may be split into two components, $\mathcal{I}(t) = \mathcal{I}_R + \mathcal{I}_C$.

The first component is the resistive current $\mathcal{I}_R$ which passes through the linear resistor R. It can be calculated from Ohm's law as $\mathcal{I}_R = u/R$ where u is the voltage applied at the resistor. The second component $\mathcal{I}_C$ charges the capacitor C. From the definition of the capacity as $C = q/u$ (where q is the charge and u the voltage), we find a capacitive current $\mathcal{I}_C = C\, du/dt$. Thus

$$\mathcal{I}(t) = \frac{u(t)}{R} + C\,\frac{du}{dt}\,. \tag{1.28}$$

We multiply (1.28) by R and introduce the time constant $\tau_m = RC$ of the 'leaky integrator'. This yields the standard form

$$\tau_m\,\frac{du}{dt} = -u(t) + R\,\mathcal{I}(t)\,. \tag{1.29}$$

We refer to u as the membrane potential and to τ_m as the membrane time constant of the neuron.

In integrate-and-fire models the form of an action potential is not described explicitly. Spikes are reduced to formal events and fully characterized by a 'firing time' $t^{(f)}$. The firing time is defined by a threshold process

$$u(t) = \vartheta \Longrightarrow t = t^{(f)}\,. \tag{1.30}$$

Immediately after $t^{(f)}$, the potential is reset to a new value $u_r < \vartheta$,

$$\lim_{\delta \to 0_+} u(t^{(f)} + \delta) = u_r\,. \tag{1.31}$$

For $t > t^{(f)}$ the dynamics is again given by (1.29) until the next threshold crossing occurs. The combination of leaky integration (1.29) and reset (1.31) defines the basic integrate-and-fire model.

4.1.1 Example: Constant stimulation and firing rates

Before we continue with the definition of the integrate-and-fire model and its variants, let us study a simple example. Let us suppose that the integrate-and-fire neuron defined by (1.29) - (1.31) is stimulated by a constant input current $\mathcal{I}(t) = \mathcal{I}_0$. To keep the mathematical steps as simple as possible we take the reset potential to be $u_r = 0$.

As a first step, let us calculate the time course of the membrane potential. We assume that a first spike has occurred at $t = t^{(0)}$. The trajectory of the membrane potential can be found by integrating (1.29) with the initial condition $u(t^{(0)}) = u_r = 0$. The solution is

$$u(t) = R\mathcal{I}_0\left[1 - \exp\left(-\frac{t - t^{(0)}}{\tau_m}\right)\right]\,. \tag{1.32}$$

The membrane potential approaches for $t \to \infty$ the asymptotic value $u(\infty) = R\mathcal{I}_0$. For $R\mathcal{I}_0 < \vartheta$ no further spike can occur. For $R\mathcal{I}_0 > \vartheta$,

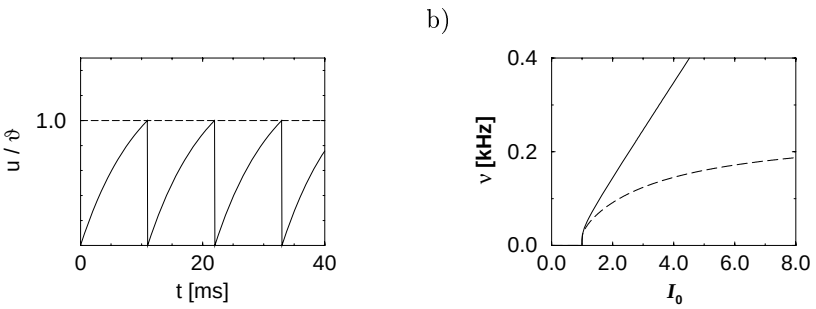

FIGURE 16. a) Time course of the membrane potential of an integrate-and-fire neuron driven by constant input current $\mathcal{I}_0 = 1.5$. The voltage $u(t)$ is normalized by the value of the threshold $\vartheta = 1$. (Resistance $R = 1$ and membrane time constant $\tau_m = 10$ ms). b) The firing rate ν of an integrate-and-fire neuron without (solid) and with absolute refractoriness of $\delta_{\rm abs} = 4$ ms (dashed) as a function of a constant driving current $\mathcal{I}_0$. Current units normalized so that the current threshold is $\mathcal{I}_\theta = 1$. (Reset to $u_r = 0$.)

the membrane potential reaches the threshold ϑ at time $t^{(1)}$, which can be found from the threshold condition $u(t^{(1)}) = \vartheta$ or

$$\vartheta = R\mathcal{I}_0 \left[1 - \exp\left(-\frac{t^{(1)} - t^{(0)}}{\tau_m}\right)\right] . \tag{1.33}$$

Solving (1.33) for the time interval $T = t^{(1)} - t^{(0)}$ yields

$$T = \tau_m \ln \frac{R\mathcal{I}_0}{R\mathcal{I}_0 - \vartheta} . \tag{1.34}$$

After the spike at $t^{(1)}$ the membrane potential is again reset to $u_r = 0$ and the integration process starts again. If the stimulus $\mathcal{I}_0$ remains constant, the following spike will occur after another interval of duration T. We conclude that for a constant input current $\mathcal{I}_0$, the integrate-and-fire neuron fires regularly with period T given by (1.34).

We may define the mean firing rate of a neuron as $\nu = 1/T$. The firing rate of the integrate-and-fire model with stimulation $\mathcal{I}_0$ is therefore

$$\nu = \left[\tau_m \ln \frac{R\mathcal{I}_0}{R\mathcal{I}_0 - \vartheta}\right]^{-1} . \tag{1.35}$$

In Fig. 16*b* the firing rate is plotted as a function of the constant input $\mathcal{I}_0$.

4.1.2 Example: Time-dependent stimulus $\mathcal{I}(t)$

The results of the preceding example can be generalized to arbitrary stimulation conditions. Let us suppose that a first spike has occurred at $\hat{t}$. For

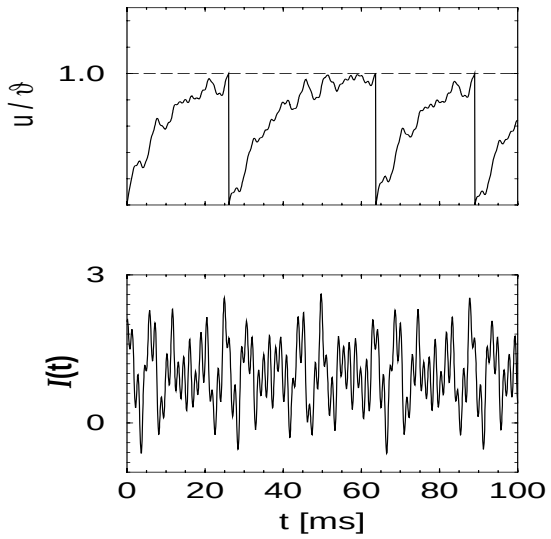

FIGURE 17. Voltage $u(t)$ of an integrate-and-fire model (top) driven by the input current $\mathcal{I}(t)$ shown at the bottom. The input $\mathcal{I}(t)$ consists of a superposition of four sinusoidal components at randomly chosen frequencies plus a positive bias current $\mathcal{I}_0 = 1.2$ which drives the membrane potential towards the threshold.

$t > \hat{t}$ the stimulating current is $\mathcal{I}(t)$. We allow for an arbitrary reset value u_r. The value u_r will be treated as an initial condition for the integration of (1.29). The formal result of the integration is

$$u(t) = u_r \exp\left(-\frac{t-\hat{t}}{\tau_m}\right) + \frac{1}{C}\int_0^{t-\hat{t}} \exp\left(-\frac{s}{\tau_m}\right) \mathcal{I}(t-s)\, ds\,. \qquad (1.36)$$

(1.36) describes the membrane potential for $t > \hat{t}$ and is valid up to the moment of the next threshold crossing. If $u(t) = \vartheta$, the membrane potential is reset to u_r and integration may restart; see Fig. 17.

4.1.3 Example: Absolute refractoriness

It is straightforward to include an absolute refractory period. After a spike at $t^{(f)}$, we force the membrane potential to a value $u = u_r$ and keep it there during a time $\delta^{\rm abs}$. Current $\mathcal{I}(t)$ which arrives during the interval $[t^{(f)}, t^{(f)} + \delta^{\rm abs}]$ has no effect and is disregarded. At $t^{(f)} + \delta^{\rm abs}$ the integration of (1.29) is restarted with the initial value $u = u_r$. The time interval $\delta^{\rm abs}$ during which the neuron is insensitive to input is called the 'absolute refractory period'.

The inclusion of an absolute refractory period does not cause any problems for the integration of the model equations. For example, we can solve

the dynamics for a constant input current $\mathcal{I}_0$. If a first spike has occurred at $t = t^{(0)}$ then $u(t) \equiv u_r$ for $t^{(0)} < t < t^{(0)} + \delta^{\rm abs}$ and

$$u(t) = R\mathcal{I}_0 \left[1 - \exp\left(-\frac{t - t^{(0)} - \delta^{\rm abs}}{\tau_m}\right)\right] + u_r \exp\left(-\frac{t - t^{(0)} - \delta^{\rm abs}}{\tau_m}\right) \tag{1.37}$$

for $t > t^{(0)} + \delta^{\rm abs}$.

If $R\mathcal{I}_0 > \vartheta$, the neuron will fire regularly. Due to the absolute refractory period the interval between firings is now longer by an amount $\delta^{\rm abs}$ compared to the value in (1.34). The mean firing rate $\nu = 1/T$ is

$$\nu = \left[\delta^{\rm abs} + \tau_m \ln \frac{R\mathcal{I}_0 - u_r}{R\mathcal{I}_0 - \vartheta}\right]^{-1} . \tag{1.38}$$

The firing rate of the integrate-and-fire neuron as a function of the constant input current is plotted in Fig. 16*b*.

4.2 Stimulation by synaptic currents

So far we have considered an isolated neuron which is stimulated by an applied current $\mathcal{I}(t)$. In a more realistic situation, the integrate-and-fire model would be part of a larger network. The input current $\mathcal{I}(t)$ is then generated by the activity of presynaptic neurons.

In the framework of the integrate-and-fire model, we may assume that each presynaptic spike generates a synaptic *current* pulse of finite width. If the presynaptic neuron j has fired at $t_j^{(f)}$, spike arrival at the synapse will evoke a current $\alpha(t - t_j^{(f)})$ for $t > t_j^{(f)}$. Since several presynaptic neurons contribute to driving the neuron, the total input current to neuron i is

$$\mathcal{I}_i(t) = \sum_{j \in \Gamma_i} c_{ij} \sum_{t_j^{(f)} \in \mathcal{F}_j} \alpha(t - t_j^{(f)}) . \tag{1.39}$$

The factor c_{ij} is a measure of the efficacy of the synapse with units of a charge.[1] (1.39) is a reasonable model of synaptic interaction. Indeed, each input spike arriving at a synapse opens some ion channels and evokes a current through the membrane of the postsynaptic neuron i.

Reality is somewhat more complicated, however, since the amplitude of the synaptic input current may itself depend on the membrane voltage u_i. In detailed models, each presynaptic action potential evokes a change in the synaptic *conductance* with standard time course $g(t - t^{(f)})$ where $t^{(f)}$ is the arrival time of the presynaptic pulse. The synaptic input current is modeled as

$$\mathcal{I}_i(t - t^{(f)}) = g(t - t^{(f)}) \, [u_i(t) - u_{\rm rev}] . \tag{1.40}$$

[1] c_{ij} is, of course, proportional to the synaptic efficacy w_{ij} as we will see later on.

The parameter $u_{\rm rev}$ is called the reversal potential of the synapse.

The level of the reversal potential depends on the type of synapse. For excitatory synapses, $u_{\rm rev}$ is much larger than the resting potential. The synaptic current then shows saturation. The higher the voltage u_i, the smaller the amplitude of the input current. The total input current is therefore not simply the sum of independent contributions. Nevertheless, since the reversal potential of excitatory synapses is usually significantly above the firing threshold, the factor $[u_i - u_{\rm rev}]$ is nearly constant and saturation can be neglected. Systematic corrections to the current equation (1.39) will be derived in section 6.

For inhibitory synapses, the reversal potential is close to the resting potential. An action potential arriving at an inhibitory synapse pulls the membrane potential towards the reversal potential $u_{\rm rev}$ which is close to $u_{\rm rest}$. Thus, if the neuron is at rest, inhibitory input hardly has any effect. If the membrane potential is instead considerably above the resting potential, then the same input has a strong inhibitory effect. This is sometimes described as the 'shunting' phenomenon of inhibition. The limitations of the current equation (1.39) will be discussed in section 6. In the following we will always work with (1.39).

4.2.1 Example: Pulse-coupling and α-function

In this subsection we will give some examples of the synaptic current $\alpha(s)$ in (1.39). We start with the simplest choice. Spikes of a presynaptic neuron j are described as Dirac δ-pulses which are fed directly into the postsynaptic neuron i. Thus $\alpha(s) = \delta(s)$. The total input *current* to unit i is then

$$\mathcal{I}_i(t) = \sum_{j\in\Gamma_i} c_{ij} \sum_{t_j^{(f)}\in\mathcal{F}_j} \delta(t - t_j^{(f)})\,. \tag{1.41}$$

As before, the factor c_{ij} is a measure of the strength of the connection from j to i. In case of (1.41), c_{ij} can be identified with the charge deposited on the capacitor C by a single presynaptic pulse of neuron j.

More realistically, the synaptic current α should have some finite width. In Fig. (15) we have sketched the situation where $\alpha(s)$ consists of a simple exponentially decaying pulse

$$\alpha(s) = \frac{1}{\tau_s} \exp\left(-\frac{s}{\tau_s}\right) \quad \text{for} \quad s > 0 \tag{1.42}$$

and zero otherwise. (1.42) is a first approximation to the low-pass characteristics of a synapse.

The exponential pulse (1.42) can be considered to be the result of some synaptic dynamics described by a first-order linear differential equation. Let us set

$$\tau_s \frac{d}{dt}\mathcal{I}_i(t) = -\mathcal{I}_i + \sum_{j\in\Gamma_i} c_{ij} \sum_{t_i^{(f)}\in\mathcal{F}_j} \delta(t - t_j^{(f)})\,. \tag{1.43}$$

Integration of the differential equation (1.43) yields (1.39) with $\alpha(s)$ given by (1.42).

In (1.42) the synaptic current has a vanishing rise time which is not very realistic. More generally, we may assume a double exponential which sets in after a transmission delay $\Delta^{\rm ax}$. For $s < \Delta^{\rm ax}$ we therefore have $\alpha(s) = 0$. For $s > \Delta^{\rm ax}$ we set

$$\alpha(s) = \frac{1}{\tau_s - \tau_r} \left[\exp\left(-\frac{s - \Delta^{\rm ax}}{\tau_s} \right) - \exp\left(-\frac{s - \Delta^{\rm ax}}{\tau_r} \right) \right] \tag{1.44}$$

Here τ_s is a synaptic time constant in the millisecond range and τ_r with $\tau_r \leq \tau_s$ is a further time constant which describes the rise time of the synaptic current pulse.

In the limit of $\tau_r \to \tau_s$, (1.44) yields (for $s > \Delta^{\rm ax}$)

$$\alpha(s) = \frac{s - \Delta^{\rm ax}}{\tau_s^2} \exp\left(-\frac{s - \Delta^{\rm ax}}{\tau_s} \right) \tag{1.45}$$

In the literature, a function of the form $x \exp(-x)$ such as (1.45) is often called an α-function. While this has motivated our choice of the symbol α for the synaptic input current, $\alpha(.)$ in (1.39) may stand for any form of an input current pulse. As mentioned before, a yet more realistic description of the synaptic input current would include a reversal potential for the synapse as defined in (1.40).

4.3 Spike Response Method (2): Reset as Current Pulse

The basic equation of the integrate-and-fire model, Eq. (1.29), is a *linear* differential equation. It can therefore be integrated in a straightforward manner. Due to the threshold and reset conditions, Eqs. (1.30) and (1.31), the integration process is not completely trivial. In fact, there are two different ways of integrating (1.29). The first one treats the reset as a current pulse, the second one as an initial condition. We discuss both methods in turn. In this subsection we focus on the first method and describe the reset as an additional current.

Let us consider for the moment a short current pulse $\mathcal{I}_i^{\rm out} = -q\,\delta(t)$ applied to the RC circuit of Fig. 15. It removes a charge q from the capacitor C and lowers the potential by an amount $\Delta u = -q/C$. Thus a reset of the membrane potential from a value of $u = \vartheta$ to a new value $u = u_r$ corresponds to a negative current pulse which removes a charge $q = C\,(\vartheta - u_r)$. Such a reset takes place at the firing time $t_i^{(f)}$. The total reset current is therefore

$$\mathcal{I}_i^{\rm out}(t) = -C\,(\vartheta - u_r) \sum_{t_i^{(f)} \in \mathcal{F}_i} \delta(t - t_i^{(f)}) \tag{1.46}$$

where the sum runs over all firing times. Formally, we may add the output current (1.46) on the right-hand side of (1.29)

$$\tau_m \frac{du_i}{dt} = -u_i(t) + R\,\mathcal{I}_i(t) + R\,\mathcal{I}_i^{\rm out}(t)\,. \tag{1.47}$$

Here

$$\mathcal{I}_i(t) = \sum_{j\in\Gamma_i} c_{ij} \sum_{t_j^{(f)}\in\mathcal{F}_j} \alpha(t-t_j^{(f)}) + \mathcal{I}_i^{\rm ext}(t) \tag{1.48}$$

is the total input current to neuron i, generated either by presynaptic spike arrival or by external stimulation $\mathcal{I}_i^{\rm ext}(t)$. Since (1.47) is a linear equation, it may be integrated. As an initial condition we take $u(-\infty) = 0$. The integration yields

$$\begin{aligned} u_i(t) &= \frac{1}{C}\int_0^\infty \exp\left(-\frac{s}{\tau_m}\right)\,\left[\mathcal{I}^{\rm out}(t-s) + \mathcal{I}_i(t-s)\right]\,ds \\ &= \sum_{t_i^{(f)}\in\mathcal{F}_i} \int_0^\infty -(\vartheta-u_r)\,\exp\left(-\frac{s}{\tau_m}\right)\,\delta(t-t_i^{(f)}-s)\,ds \\ &\quad + \sum_{j\in\Gamma_i}\sum_{t_j^{(f)}\in\mathcal{F}_j} \int_0^\infty \frac{c_{ij}}{C}\,\exp\left(-\frac{s}{\tau_m}\right)\,\alpha(t-t_j^{(f)}-s)\,ds \\ &\quad + \frac{1}{C}\int_0^\infty \exp\left(-\frac{s}{\tau_m}\right)\,\mathcal{I}_i^{\rm ext}(t-s)\,ds \end{aligned} \tag{1.49}$$

Let us define for $s > 0$

$$\eta_0(s) = -(\vartheta-u_r)\,\exp\left(-\frac{s}{\tau_m}\right) \tag{1.50}$$

$$\epsilon_0(s) = \int_0^\infty \exp\left(-\frac{s'}{\tau_m}\right)\,\alpha(s-s')\,ds' \tag{1.51}$$

$$\tilde{\epsilon}_0(s) = \frac{1}{C}\,\exp\left(-\frac{s}{\tau_m}\right) \tag{1.52}$$

and $\eta_0(s) = \epsilon_0(s) = \tilde{\epsilon}_0(s) = 0$ for $s < 0$. With the above definitions, (1.49) may be rewritten in the form

$$\begin{aligned} u_i(t) &= \sum_{t_i^{(f)}\in\mathcal{F}_i} \eta_0(t-t_i^{(f)}) + \sum_{j\in\Gamma_i} w_{ij} \sum_{t_j^{(f)}\in\mathcal{F}_j} \epsilon_0(t-t_j^{(f)}) \\ &\quad + \int_0^\infty \tilde{\epsilon}_0(s)\,\mathcal{I}_i^{\rm ext}(t-s)\,ds\,. \end{aligned} \tag{1.53}$$

with weights $w_{ij} = c_{ij}/C$. Eq. (1.53) is the main result of this subsection. The kernel $\eta_0(s)$ defined by (1.50) is shown in Fig. 18.

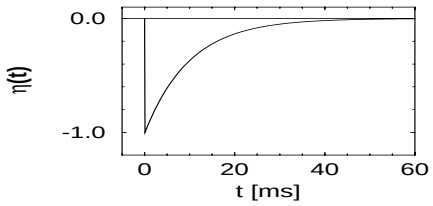

FIGURE 18. The kernel η_0 of the integrate-and-fire model with membrane time constant $\tau_m = 10\,\mathrm{ms}$.

We emphasize that the firing times $t_i^{(f)}$ which appear implicitly in (1.49) have to be calculated as before from the threshold condition $u_i(t) = \vartheta$. In [GvHC96], the 'Spike Response Model' has been *defined* by (1.53). Note that, in contrast to (1.15), we still have a sum over past spikes of neuron i on the right-hand-side of (1.53).

4.3.1 Examples of ϵ_0-kernels

If $\alpha(s)$ is given by (1.42), then the integral on the right-hand side of (1.51) can be done and yields ($s > 0$)

$$\epsilon_0(s) = \frac{1}{1-(\tau_s/\tau_m)} \left[\exp\left(-\frac{s}{\tau_m}\right) - \exp\left(-\frac{s}{\tau_s}\right)\right] . \tag{1.54}$$

This is the ϵ kernel shown in Fig. 19a. If $\alpha(s)$ is the Dirac δ-function, then we find simply $\epsilon_0(s) = \exp(-s/\tau_m)$ as shown in Fig. 19*b*.

Note that $\alpha(s)$ is the synaptic *current*. Integration of the synaptic current yields the postsynaptic *potential* $\epsilon_0(s)$. If the synapse is excitatory, ϵ_0 is called the excitatory postsynaptic potential (EPSP). For an inhibitory synapse, ϵ_0 describes the inhibitory postsynaptic potential (IPSP).

4.3.2 Short-term memory approximation

To keep the discussion transparent, let us set $\mathcal{I}_i^{\rm ext} = 0$. Eq. (1.53) is then

$$u_i(t) = \sum_{t_i^{(f)} \in \mathcal{F}_i} \eta_0(t - t_i^{(f)}) + \sum_{j \in \Gamma_i} w_{ij} \sum_{t_j^{(f)} \in \mathcal{F}_j} \epsilon_0(t - t_j^{(f)}) . \tag{1.55}$$

On the right-hand side of (1.55), there is a sum over all past firings of neuron i which does not appear in (1.15), the equation we are aiming for.

According to (1.50) the effect of the η_0-kernel decays with a time constant τ_m. In realistic spike trains, the interval between two spikes is typically much longer than the membrane time constant τ_m. Hence the sum over the η_0 terms is usually dominated by the *most recent* firing time $t_i^{(f)} < t$ of neuron i. We therefore make a truncation and neglect the effect of earlier

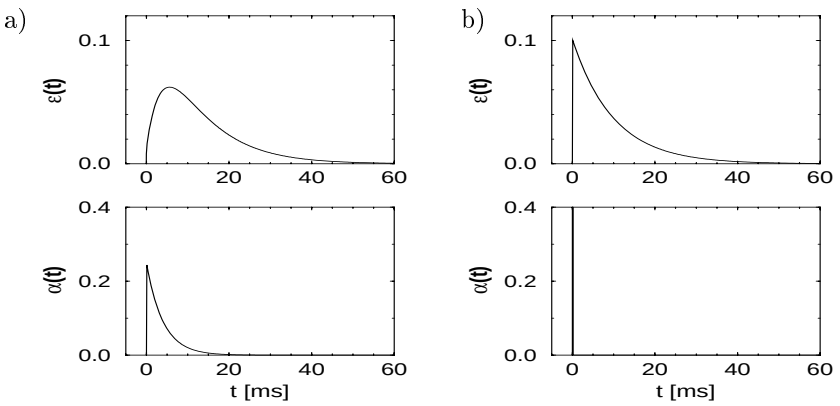

FIGURE 19. a) ϵ-kernel of the integrate-and-fire model (top) with exponential synaptic input current α (bottom). b) If the synaptic input is pulse-like (bottom), then the ϵ-kernel is a simple exponential.

spikes

$$\sum_{t_i^{(f)} \in \mathcal{F}_i} \eta_0(t - t_i^{(f)}) \longrightarrow \eta_0(t - \hat{t}_i) \tag{1.56}$$

where $\hat{t}_i$ is the last firing time of neuron i. The approximation (1.56) is good if the mean firing rate of the neuron is low, i.e., if the intervals between two spikes are much longer than τ_m. Loosely speaking, we may say that the neuron remembers only its most recent firing. (1.56) may therefore be called a 'short-term memory approximation' [GvHC96]. The final equation is

$$u_i(t) = \eta_0(t - \hat{t}_i) + \sum_{j \in \Gamma_i} w_{ij} \sum_{t_j^{(f)} \in \mathcal{F}_j} \epsilon_0(t - t_j^{(f)}) \,. \tag{1.57}$$

This is exactly the equation for the model SRM_0, defined in (1.20). Note that we have kept, on the right-hand side of (1.57), the sum over all *presynaptic* firing times $t_j^{(f)}$. Only the sum over the η_0's has been truncated.

Eq. (1.57) can be seen as an approximation to the integrate-and-fire model or else as a model in its own rights. The advantage of SRM_0 is that many network results can be derived in a rather transparent manner [Ger95, GvHC96, Ger00]. Moreover questions of computation and coding with spiking neurons can be analyzed in the context of SRM_0 [Maa96, Maa98, Ger98].

4.4 Spike Response Method (3): Reset as Initial Condition

In this section, we discuss a method of integration which gives a direct mapping of the integrate-and-fire model

$$\tau_m \frac{du_i}{dt} = -u_i(t) + R \sum_{j\in\Gamma_i} c_{ij} \sum_{t_j^{(f)}\in\mathcal{F}_j} \alpha(t-t_j^{(f)}) + \mathcal{I}_i^{\rm ext}(t) \tag{1.58}$$

to the Spike Response Model (1.15). As in (1.36) we integrate (1.58) from $\hat{t}_i$ to t with $u(\hat{t}_i) = u_r$ as an initial condition. The result is

$$\begin{aligned} u(t) &= u_r \exp\left(-\frac{t-\hat{t}_i}{\tau_m}\right) \\ &\quad + \sum_{j\in\Gamma_i} \sum_{t_j^{(f)}\in\mathcal{F}_j} \frac{c_{ij}}{C} \int_0^{t-\hat{t}_i} \exp\left(-\frac{s'}{\tau_m}\right) \alpha(t-t_j^{(f)}-s')\, ds' \\ &\quad + \frac{1}{C}\int_0^{t-\hat{t}_i} \exp\left(-\frac{s'}{\tau_m}\right) \mathcal{I}_i^{\rm ext}(t-s')\, ds' \end{aligned} \tag{1.59}$$

We may now define kernels

$$\eta(t-\hat{t}_i) = u_r \exp\left(-\frac{t-\hat{t}_i}{\tau_m}\right) \tag{1.60}$$

$$\epsilon(t-\hat{t}_i, s) = \int_0^{t-\hat{t}_i} \exp\left(-\frac{s'}{\tau_m}\right) \alpha(s-s')\, ds' \tag{1.61}$$

$$\tilde{\epsilon}(t-\hat{t}_i, s) = \frac{1}{C} \exp\left(-\frac{s}{\tau_m}\right) \mathcal{H}(t-\hat{t}_i-s) \tag{1.62}$$

and the synaptic efficacy $w_{ij} = c_{ij}/C$. As usual, $\mathcal{H}(x)$ denotes the Heaviside step function which vanishes for $x \le 0$ and has a value of one for $x > 0$. The kernels (1.60) - (1.61) allow us to rewrite (1.59) in the form

$$\begin{aligned} u_i(t) &= \eta_i(t-\hat{t}_i) + \sum_{j\in\Gamma_i} w_{ij} \sum_{t_j^{(f)}\in\mathcal{F}_j} \epsilon(t-\hat{t}_i, t-t_j^{(f)}) \\ &\quad + \int_0^\infty \tilde{\epsilon}(t-\hat{t}_i, s)\, \mathcal{I}_i^{\rm ext}(t-s)\, ds \end{aligned} \tag{1.63}$$

which is identical to (1.15) except for some minor changes of notation. We emphasize that the η-kernel defined in (1.60) is not the same as the one defined in (1.50). In particular, the η-kernel (1.60) vanishes if $u_r = 0$.

4.4.1 Examples of ϵ kernels

In order to calculate the ϵ kernels (1.61) and (1.62) explicitly, it is convenient to distinguish two cases. First we consider the case, that the last

output spike occurred *before* presynaptic spike arrival ($\hat{t}_i < t_j^{(f)}$). Therefore $t-\hat{t}_i > t-t_j^{(f)} = s$. Since $\alpha(s-s')$ vanishes for $s-s' < 0$ we may extend the upper boundary in (1.61) to infinity without introducing an error. Hence, for $t_j^{(f)} > \hat{t}_i$, we have $\epsilon(t-\hat{t}_i, t-t_j^{(f)}) = \epsilon_0(t-t_j^{(f)})$ where ϵ_0 has been defined in (1.51).

The situation is different, if $\hat{t}_i > t_j^{(f)}$, i.e., if the last output spike has occurred *after* presynaptic spike arrival. In this case only that part of the synaptic current which arrives after $\hat{t}_i$ contributes to the present postsynaptic potential and

$$\epsilon(t-\hat{t}_i, t-t_j^{(f)}) = \int_{\hat{t}_i}^{t} \exp\left(-\frac{t-t'}{\tau_m}\right) \alpha(t'-t_j^{(f)})\, dt' \tag{1.64}$$

To be specific, we take $\alpha(s)$ as defined in (1.42), viz.,

$$\alpha(s) = \tau_s^{-1} \exp\left(-s/\tau_s\right) \mathcal{H}(s)\,. \tag{1.65}$$

Let us set $x = t-\hat{t}_i$. The integration of (1.61) yields [Ger95]

$$\begin{aligned} \epsilon(x,s) &= \frac{1}{1-\frac{\tau_s}{\tau_m}} \left\{ \left[\exp\left(-\frac{s}{\tau_m}\right) - \exp\left(-\frac{s}{\tau_s}\right)\right] \mathcal{H}(s)\,\mathcal{H}(x-s) \right. \\ &+ \left. \exp\left(-\frac{s-x}{\tau_m}\right) \left[\exp\left(-\frac{x}{\tau_m}\right) - \exp\left(-\frac{x}{\tau_s}\right)\right] \mathcal{H}(x)\,\mathcal{H}(s-x) \right\} \end{aligned} \tag{1.66}$$

The Heaviside functions $\mathcal{H}(x-s)$ in the first line of (1.66) picks out the case $t_j^{(f)} > \hat{t}_i$ or $x > s$. The second line contains the factor $\mathcal{H}(s-x)$ and applies to the case $t_j^{(f)} < \hat{t}_i$ or $x < s$. See Fig. 20 for an illustration of the result.

4.4.2 Transformation of the ϵ kernel

What is the relation between the ϵ kernel derived in (1.61) and the ϵ_0 introduced in (1.51)? We will show in this paragraph that

$$\epsilon(x,s) = \epsilon_0(s) - \exp\left(-\frac{x}{\tau_m}\right) \epsilon_0(s-x) \tag{1.67}$$

holds. To see how this comes about we start from (1.61). We set $x = t-\hat{t}_i$ and $y = s-s'$ and find

$$\begin{aligned} \epsilon(x,s) &= \int_{s-x}^{s} \exp\left(-\frac{s-y}{\tau_m}\right) \alpha(y)\, dy \\ &= \int_{-\infty}^{s} \exp\left(-\frac{s-y}{\tau_m}\right) \alpha(y)\, dy - \int_{-\infty}^{s-x} \exp\left(-\frac{s-y}{\tau_m}\right) \alpha(y)\, dy \end{aligned} \tag{1.68}$$

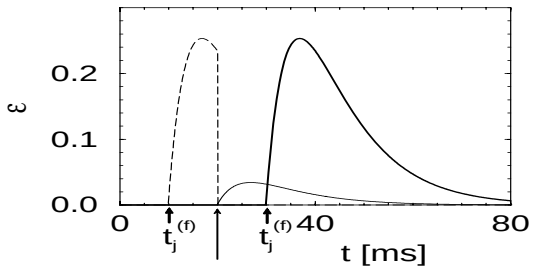

FIGURE 20. The kernel $\epsilon(t-\hat{t}, t-t_j^{(f)})$ as a function of t for two different situations. If $t_j^{(f)} > \hat{t}$, then $\epsilon(t-\hat{t}, t-t_j^{(f)}) = \epsilon_0(t-t_j^{(f)})$ is the standard EPSP (thick solid line). If $t_j^{(f)} < \hat{t}$, the amplitude of the EPSP for $t > \hat{t}$ is much smaller (thin solid line) since the time course of the EPSP is 'reset' to zero at $t = \hat{t}$ (marked by the long arrow). The time couse for $t < \hat{t}$ is indicated by the dashed line.

In the first term on the right-hand side of (1.68) we may transform back to the variable $s' = s - y$, in the second term we set $s' = s - x - y$. This yields

$$\begin{aligned}\epsilon(x,s) &= \int_0^\infty \exp\left(-\frac{s'}{\tau_m}\right)\,\alpha(s-s')\,ds' \\ &\quad - \exp\left(-\frac{x}{\tau_m}\right)\,\int_0^\infty \exp\left(-\frac{s'}{\tau_m}\right)\,\alpha(s-x-s')\,ds' \\ &= \epsilon_0(s) - \exp\left(-\frac{x}{\tau_m}\right)\,\epsilon_0(s-x)\,. \end{aligned} \tag{1.69}$$

The last equality follows from the definition of ϵ_0 in (1.51).

By a completely analogous sequence of transformations it is possible to show that

$$\tilde{\epsilon}(x,s) = \tilde{\epsilon}_0(s) - \exp\left(-\frac{x}{\tau_m}\right)\,\tilde{\epsilon}_0(s-x)\,. \tag{1.70}$$

The total postsynaptic potential $h_{\rm PSP}$ defined in (1.17) can therefore be expressed via the input potential h_i [Ger00]

$$h_{\rm PSP}(t|\hat{t}_i) = h_i(t) - \exp\left(-\frac{t-\hat{t}_i}{\tau_m}\right)\,h_i(\hat{t}_i) \tag{1.71}$$

As it should be expected, the reset at $\hat{t}_i$ has an influence on the total postsynaptic potential. We emphasize that the expressions (1.69) - (1.71) hold for the integrate-and-fire model only. For a general Hodgkin-Huxley type dynamics the transformations discussed in this paragraph would not be possible.

4.4.3 Relation between the two integration methods

In order to better understand the relation between the two integration methods outlined in sections 4.3 and 4.4, we compare the η-kernel in (1.60) with the η_0-kernel defined in (1.50):

$$\begin{aligned} \eta(s) &= u_r \exp\left(-\frac{s}{\tau_m}\right) \\ &= \eta_0(s) + \vartheta \exp\left(-\frac{s}{\tau_m}\right) . \end{aligned} \tag{1.72}$$

Hence with (1.71), the potential is

$$\begin{aligned} u_i(t) &= \eta(t-\hat{t}_i) + h_{\rm PSP}(t|\hat{t}_i) \\ &= \eta_0(t-\hat{t}_i) + h(t) - [h(\hat{t}_i) - \vartheta] \exp\left(-\frac{t-\hat{t}_i}{\tau_m}\right) . \end{aligned} \tag{1.73}$$

The truncation in (1.56) is therefore equivalent to neglecting the last term in (1.73).

4.5 Discussion

The second of the two integration methods shows that it is possible to map the integrate-and-fire model exactly to the spike response equation (1.15). The disadvantage of that method is that the ϵ kernels look somwhat more complicated. This is, however, no real drawback since the dynamics of a population of spiking neurons can be discussed for *arbitrary* response kernels η and ϵ [Ger95, Ger00]. The integrate-and-fire model is therefore a special case in the general framework of the spike response model.

With the first method of integration, the mapping of the integrate-and-fire model to (1.15) is only approximate. The approximation is good if the typical interspike interval is long compared to the membrane time constant τ_m. The main advantage of the approximation is that the ϵ kernels do not depend on the state of the postsynaptic neuron. Therefore the input potential $h_i(t)$ can be nicely separated from the effects of reset and refractoriness; cf. (1.26) and (1.27). The resulting model SRM_0 allows us to discuss dynamic effects in a transparent graphical manner; see, e.g., [GvHC96, Ger98, Maa96, Maa98].

The basic integrate-and-fire model is, of course, a rather simple description of neuronal firing. In particular, the neuron has no spatial structure and firing is given by an explicit threshold condition. In the following section we will extend the framework (1.15) to neuron models with spatial structure.

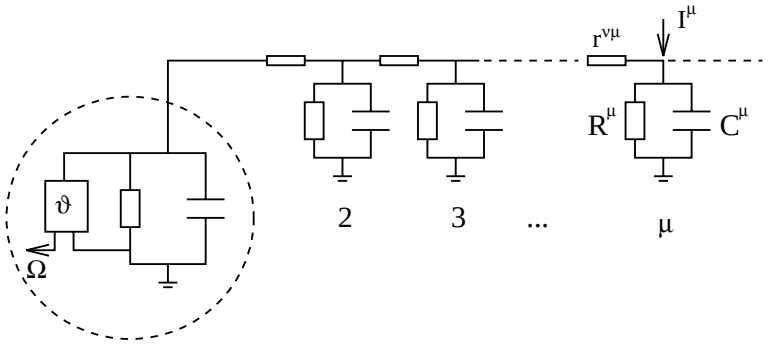

FIGURE 21. *Compartmental neuron model.* Dendritic compartments with membrane capacitance C^μ and resistance R^μ are coupled by a longitudinal resistance $r^{\nu\mu}$. Each compartment receives an input $\mathcal{I}^\mu$. The soma ($\mu = 1$) emits an output current pulse $\Omega(t)$, if the membrane potential reaches the threshold ϑ.

5 Multi-compartment model

5.1 Definition of the model

In this section, the integrate-and-fire model introduced in section 4 is generalized in two respects. First, we allow for some spatial structure and consider a neuron consisting of several compartments. Second, we refine the reset procedure and include, at the somatic compartment, additional spike currents which generate an action potential.

5.1.1 Linear dendritic tree

We consider a model with $n-1$ dendritic compartments $2 \leq \mu \leq n$ and a threshold unit at the soma ($\mu = 1$); cf. Fig. 21. Membrane resistance and capacity are denoted by R^μ and C^μ, respectively. The longitudinal core resistance between compartment μ and a neighboring compartment ν is $r^{\mu\nu}$. We assume a common time constant $R^\mu C^\mu = \tau_0$ for all compartments $1 \leq \mu \leq n$. The above specifications define the standard model of a linear dendrite [Ral89].

Each compartment $1 \leq \mu \leq n$ receives input $I^\mu(t)$ from some presynaptic neurons. At the soma, there is an additional current $\Omega(t)$ due to action potential generation. The change of the membrane potential V^μ of compartment μ is

$$C^\mu \frac{d}{dt} V^\mu = -\frac{V^\mu}{R^\mu} + \sum_\nu \frac{V^\mu - V^\nu}{r^{\mu\nu}} + I^\mu(t) - \delta^{\mu\,1}\Omega(t) \tag{1.74}$$

where the sum runs over all neighbors of compartment μ.

5.1.2 Synaptic input

The input $I^\mu(t)$ in (1.74) is due to spikes of those presynaptic neurons with synapses on compartment μ of neuron i. The set of these neurons is denoted by Γ^μ. As before in (1.39), we assume that each spike evokes a current pulse of standard form $\alpha(t-t_j^{(f)})$ with $\alpha(s)=0$ for $s<0$. The amplitude of the current pulse is scaled by c_{ij} where i is the index of the postsynaptic neuron. The total input to compartment μ of neuron i is

$$I_i^\mu(t) = \sum_{j\in\Gamma^\mu} c_{ij} \sum_{t_j^{(f)}\in\mathcal{F}_j} \alpha(t-t_j^{(f)}). \tag{1.75}$$

Choices for $\alpha(s)$ have already been discussed in section 4.2.

5.1.3 Spike currents

Neuron i fires, if the somatic membrane potential $V_i^1(t)$ reaches a threshold ϑ. More precisely, a firing time $t_i^{(f)}$ is defined by the conditions $V_i^1(t_i^{(f)})=\vartheta$ and $\frac{d}{dt}V_i^1(t_i^{(f)})>0$. Each firing consists of a short current pulse $\gamma(t-t_i^{(f)})$ at the soma [Abe91, GvHC96, SNS95]. The total 'output' current of neuron i is

$$\Omega_i(t) = -\sum_{t_i^{(f)}\in\mathcal{F}_i} \gamma(t-t_i^{(f)}). \tag{1.76}$$

Due to causality, $\gamma(s)$ vanishes for $s<0$.

The pulse $\gamma(s)$ describes the typical time course of sodium and potassium currents (and possibly calcium currents) during and after an action potential. Typically, $\gamma(s)$ is large and positive during the rise time of the spike and $\gamma(s)$ is non-positive thereafter. In principle, $\gamma(s)$ may also contain an additional phase of late depolarizing calcium currents. In general, the time course of sodium, potassium, and calcium currents depends on the stimulation before and after action potential generation. In the approximation of (1.76), this dependence is neglected and we assume a standard current pulse with *identical* time course for each firing. This is the central assumption of our approach. As we have seen in (1.46), the reset in integrate-and-fire units is equivalent to the emission of a current pulse $\gamma(s)=-q\,\delta(s)$ where $\delta(s)$ is the Dirac δ-function.

5.1.4 Example of spike currents

Let us study a specific example. We consider the case of two current sources

$$\gamma(s) = I_{\rm Na}(s) + I_{\rm K}(s) \tag{1.77}$$

which contribute to the action potential. We take

$$I_{\rm Na}(s) \;=\; q_{\rm Na}\,\frac{1}{\tau_{\rm Na}}\,\exp\left(-\frac{s}{\tau_{\rm Na}}\right) \tag{1.78}$$

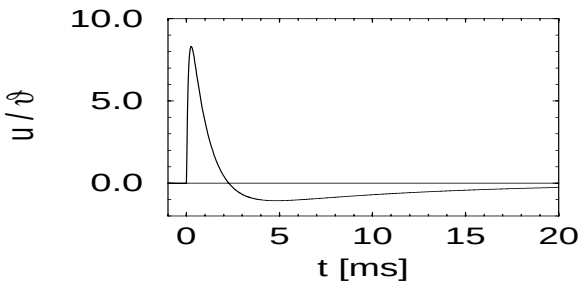

FIGURE 22. *Action potential.* Integration of the integrate-and-fire model with a spike current $\gamma(s)$ given by (1.77) yields the time course of an action potential.

$$I_{\rm K}(s) \quad = \quad q_{\rm K}\,\frac{1}{\tau_{\rm K}}\,\exp\left(-\frac{s}{\tau_{\rm K}}\right)\,[1-\exp\left(-\gamma\,s\right)] \tag{1.79}$$

with $\tau_{\rm Na} = 0.1$ ms, $\tau_{\rm K} = 1$ ms and $\gamma = 5/$ms, $q_{\rm Na} = 100$, $q_{\rm K} = -133$. For the sake of simplicity, we consider the somatic compartment only. Integration of $\tau_m du/dt = -u + R\,\gamma(t)$ with initial condition $u(0) = \vartheta$ with $R = 1$, $\vartheta = 1$, $\tau_m = 10\,$ms yields the action potential shown in Fig. (22). Note that the current time constant $\tau_{\rm Na} = 0.1\ ms$ and $\tau_{\rm K} = 1$ ms are extremely short. These are heuristic values which have been chosen so as to yield upon integration a nice shape similar to a real action potential; see [Abe91, SNS95] for related examples.

5.2 Spike Response Method -(4)

Eq. (1.74) is a system of linear differential equations. It can be integrated either for a finite number of compartments [Tuc88, BT94] or in the continuum limit [Tuc88, AFG91]. As initial conditions we take $V^\mu(-\infty) = 0$ for all compartments $1 \le \mu \le n$. The result of the integration is of the form

$$V^\mu(t) = \frac{1}{C^\mu}\sum_\nu \int_0^\infty ds' G^{\mu\nu}(s')\left[I^\nu(t-s') - \delta^{\nu 1}\Omega(t-s')\right]. \tag{1.80}$$

An explicit expression for the Greens function $G^{\mu\nu}(s)$ for arbitrary geometry can be found in [AFG91, BT94]. In order to proceed further we use Eqs. (1.76) and (1.75) and find

$$V^\mu(t) = \sum_{t_i^{(f)}\in\mathcal{F}_i} \eta^\mu(t-t_i^{(f)}) + \sum_\nu \sum_{j\in\Gamma^\nu} w_{ij} \sum_{t_j^{(f)}\in\mathcal{F}_j} \epsilon^{\mu\nu}(t-t_j^{(f)}). \tag{1.81}$$

with

$$\epsilon^{\mu\nu}(s) \quad = \quad \frac{1}{C^\mu}\int_0^\infty G^{\mu\nu}(s')\alpha(s-s')ds' \tag{1.82}$$

$$\eta^{\mu}(s) \quad = \quad \frac{1}{C^{\mu}} \int_0^{\infty} G^{\mu 1}(s') \gamma(s-s') ds'. \tag{1.83}$$

The kernel $\epsilon^{\mu\nu}(s)$ describes the effect of an input spike to compartment ν as seen at compartment μ. Similarly, $\eta^{\mu}(s)$ describes the response of compartment μ to an output spike at the soma.

To proceed further, we note that firing depends on the *somatic* membrane potential only. We define $u_i = V^1$, $\eta_0(s) = \eta^1(s)$ and, for $j \in \Gamma^{\nu}$, we set $\epsilon_{ij} = \epsilon^{1\nu}$. This yields

$$u_i(t) = \sum_{t_i^{(f)} \in \mathcal{F}_i} \eta_0(t - t_i^{(f)}) + \sum_j w_{ij} \sum_{t_j^{(f)} \in \mathcal{F}_j} \epsilon_{ij}(t - t_j^{(f)}). \tag{1.84}$$

As in (1.56), we now make a short-term memory approximation and truncate the sum over the η-terms. The result is

$$u_i(t) = \quad \eta_0(t - \hat{t}_i) + \sum_j w_{ij} \sum_{t_j^{(f)} \in \mathcal{F}_j} \epsilon_{ij}(t - t_j^{(f)}). \tag{1.85}$$

where $\hat{t}_i$ is the last firing time of neuron i. Thus, the multi-compartment model has been reduced to the single-variable model of Eq. (1.20). The approximation is good, if the typical interspike interval is long compared to the neuronal time constants.

5.2.1 Improvement of the approximation

Note that the steps taken in the previous paragraph correspond to the first of the two integration methods discussed in section 4. The second method which yields an improved mapping to the spike response model can be used as an alternative. In order to apply the second method, we must take care to correctly include the initial conditions $V^{\mu}(\hat{t}_i)$ for all compartments. Only at the soma, an explicit initial condition $V^1(\hat{t}_i) = \vartheta$ is available. In analogy to (1.69), we aim for an expression for the kernels $\epsilon(t - \hat{t}_i, t - t_j^{(f)})$ in terms of the kernel ϵ_0.

Let us start the integration of the voltage at the somatic compartment ($u_i = V^1$) at time $t = \hat{t}_i$

$$\begin{aligned} u_i(t) \quad = \quad & \int_{\hat{t}_i}^{t} G^{11}(t-t')\, \gamma(t' - \hat{t}_i)\, dt' + \sum_{t_i^{(f)} < \hat{t}_i} \int_{\hat{t}_i}^{t} G^{11}(t-t')\, \gamma(t' - t_i^{(f)})\, dt' \\ & + \sum_{\nu} \sum_{j \in \Gamma_{\nu}} \int_{\hat{t}_i}^{t} G^{1\nu}(t-t')\, \alpha(t' - t_j^{(f)})\, dt' \\ & + V^1(\hat{t}_i)\, G^{11}(t - \hat{t}_i) + \sum_{\mu \geq 2} V^{\mu}(\hat{t}_i)\, G^{1\mu}(t - \hat{t}_i)\,. \end{aligned} \tag{1.86}$$

The terms in the last line of (1.86) are the initial conditions for the compartment voltages. For the somatic compartment, we use $V^1(\hat{t}_i) = \vartheta$. For $\mu \geq 2$ we may formally use (1.81) evaluated at $t = \hat{t}_i$. The sum in the first line on the right-hand side of (1.86) vanishes if the spike currents have stopped before the next spike occurs – as it is trivially the case for a reset current $\gamma(s) = -q\delta(s)$. In the following we will therefore neglect these terms.

We now define

$$\eta(t - \hat{t}_i) = \eta_0(t - \hat{t}_i) + \vartheta\, G^{11}(t - \hat{t}_i) \tag{1.87}$$

and, for $j \in \Gamma_\nu$

$$\epsilon_{ij}(t - \hat{t}_i, t - t_j^{(f)}) = \epsilon^{1\nu}(t - t_j^{(f)}) - G^{11}(t - \hat{t}_i)\, \epsilon^{1\nu}(\hat{t}_i - t_j^{(f)}) \tag{1.88}$$

We use $G^{1\nu}(x + y) = \sum_\mu G^{1\mu}(x)\, G^{\mu\nu}(y)$ in the Greens function in the second line of (1.86). With (1.87) and (1.88) we find after some calculation:

$$\begin{aligned} u_i(t) &= \eta(t - \hat{t}_i) + \sum_j w_{ij} \sum_{t_j^{(f)} \in \mathcal{F}_j} \epsilon_{ij}(t - \hat{t}, t - t_j^{(f)}) \\ &\quad + \sum_{\mu \geq 2} G^{1\mu}(t - \hat{t}_i) \sum_{t_i^{(f)} < \hat{t}_i} \eta^\mu(t - t_i^{(f)})\,. \end{aligned} \tag{1.89}$$

In order to get a mapping to (1.15) we need to suppress the terms in the second line of (1.89). These are terms which describe the effect of previous output spikes of neuron i on the dendritic compartment ν and which cause now for $t > \hat{t}_i$ some feedback onto the soma.

Note the close analogy between (1.88) and (1.69). The Greens function G^{11} is the generalization of the exponential term in (1.69). Similarly, the η-kernel (1.87) is the generalization of (1.72). We emphasize that for a single-compartment model, the sum in the last line of (1.89) vanishes. The mapping between the integrate-and-fire model and the spike response model (1.15) is then exact, as we have seen in section 4.4. For a multi-compartment model the mapping to (1.15) is not exact. The approximation derived in this paragraph is, however, better than the truncation that is necessary to get (1.85).

5.2.2 Example: Two-compartment integrate-and-fire model

We illustrate the Spike Response Method by a simple model with two compartments and a reset mechanism at the soma. The two compartments are characterized by a somatic capacitance C^1 and a dendritic capacitance $C^2 = a\, C^1$. The membrane time constant is $\tau_0 = R^1 C^1 = R^2 C^2$ and the longitundinal time constant $\tau_{12} = r^{12}\, \frac{C^1 C^2}{C^1 + C^2}$. The neuron fires, if $V^1 = \vartheta$. After each firing the somatic potential is reset to $V^1 = u_r$. This is equivalent to a current pulse

$$\gamma(s) = -q\, \delta(s) \tag{1.90}$$

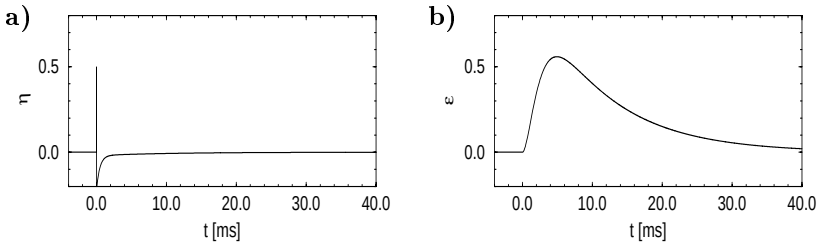

FIGURE 23. *Two-compartment integrate-and-fire model.* (a) Response kernel $\eta(s)$ of a neuron with two compartments and a fire-and-reset threshold dynamics. The response kernel is a double exponential with time constants $\tau_{12} = 2$ ms and $\tau_0 = 10$ ms. The spike at $s = 0$ is indicated by a vertical dash. (b) Response kernel $\epsilon(s)$ for excitatory synaptic input at the dendritic compartment with a synaptic time constant $\tau_s = 1$ ms. The response kernel exhibits the typical time course of an excitatory postsynaptic potential. (y-axis: voltage in arbitrary units.)

where $q = C^1 [\vartheta - u_r]$ is the charge lost during the spike. The dendrite receives spike trains from other neurons j and we assume that each spike evokes a current pulse $\alpha(t - t_j^{(f)})$ with time course

$$\alpha(s) = \frac{1}{\tau_s} \exp(-\frac{t}{\tau_s}). \tag{1.91}$$

For the two-compartment model it is straightforward to integrate the equations and derive the response kernels $\eta(s)$ and $\epsilon(s)$; cf. [Tuc88, BT94, RL93]. We find

$$\begin{aligned} \eta_0(s) &= -\frac{\vartheta - u_r}{(1+a)} \exp\left(-\frac{s}{\tau_0}\right) \left[1 + a \exp\left(-\frac{s}{\tau_{12}}\right)\right] \\ \epsilon_0(s) &= \frac{1}{(1+a)} \exp\left(-\frac{s}{\tau_0}\right) \left[\frac{1 - e^{-\delta_1 s}}{\tau_s \, \delta_1} - \exp\left(-\frac{s}{\tau_{12}}\right) \frac{1 - e^{-\delta_2 s}}{\tau_s \, \delta_2}\right] \end{aligned} \tag{1.92}$$

with $\delta_1 = \tau_s^{-1} - \tau_0^{-1}$ and $\delta_2 = \tau_s^{-1} - \tau_0^{-1} - \tau_{12}^{-1}$. In Fig. 23 we show the two response kernels for the parameters $\tau_0 = 10$ ms, $\tau_{12} = 2$ ms, and $a = 10$. The synaptic time constant is $\tau_s = 1$ ms. The kernel $\epsilon_0(s)$ describes the voltage response of the soma to an input at the dendrite. It shows the typical time course of an excitatory or inhibitory postsynaptic potential. The time course of the kernel $\eta(s)$ is a double exponential and reflects the dynamics of the reset in a two-compartment model. In Fig. 23*a*, the moment of spike firing at $t = 0$ has been marked by a vertical bar for the sake of better visibility.

6 Extensions and Discussion

The strict application of the spike response method requires a system of linear differential equations combined with a threshold process - such as

in the integrate-and-fire model in section 4. Naturally the question arises how well real neurons fit into this framework. As an example of a more complicated neuron model we have discussed the effects of a linear dendritic tree. We have also seen in section 2 that, for the Hodgkin-Huxley model, spike generation can be replaced approximatively by a threshold process. In this section we want to continue our discussion and hint to possible extensions and modifications. To check the validity of the approach, we discuss the two basic assumptions, viz., threshold process and linearity.

6.1 Threshold process

The dynamics of spike generation can be desribed by nonlinear differential equations of the type proposed by Hodgkin and Huxley [HH52]. Spikes are generated by a voltage-instability of the conductivity. Since the opening and closing of Na and K channels are described by three variables with three different time constants, the threshold depends not only on the present voltage, but also on the voltage in the recent past. In other words, there is no sharp voltage threshold [RE89, KpBD95]. This is most easily seen in a scenario with arbitrary time-dependent input. Let us suppose that, for some ion-based neuron model, there exists a voltage threshold ϑ. Even if the potential were already slightly above the formal threshold, there could arrive, in the next moment, a very strong inhibitory current which pulls the potential back below threshold. Thus spiking could still be stopped even though the action potential was already initiated. This consideration points to the general limitations of the threshold concept in the context of time-dependent stimulation. Strictly speaking there can be neither a voltage nor a current threshold if we allow for arbitrary input.

Nevertheless, an improvement over the simple voltage threshold is possible. The spike response method does not rely on a specific interpretation of the variable $u(t)$. In principle, it can be any relevant variable, e.g., a current [Rot94, KpBD95], a voltage, or some combination of current and voltage variables. To be specific, we may take

$$u(t) = \int_0^\infty f(s)\, V^1(t-s) ds = f * V^1 \tag{1.93}$$

where V^1 is the voltage at the soma and f some linear filter with normalization $\int_0^\infty f(s) ds = 1$. Since everything is linear, the response kernels derived in the preceding sections can be transformed $\epsilon \longrightarrow f * \epsilon$ and $\eta \longrightarrow f * \eta$ and we are back to the standard form (1.15). Application of the linear operator f on the voltage u in (1.8) before it is passed through a threshold would, for example, allow us to match the boundaries in the phase diagram of Fig. 5*c* more closely to that of the Hodgkin-Huxley model in Fig. 5*b*.

We emphasize that the formal threshold is constant in our approach. A dynamic threshold $\tilde{\vartheta}(t)$ which is increased after each spike [MO74] may

always be treated as an additional contribution to the respone kernel $\eta(s)$ as discussed in (1.27).

6.2 Adaptation

In all the discussion above we have assumed that only the *last* output spike of the neuron is relevant. This is, of course, an over-simplification of reality. For most neurons, adaptation plays an important role. If a constant input is switched on at t_0, the interspike interval between the first and second spike is usually shorter than the one between the 10th and eleventh.

How can adaptation be included in the above framework? One possibility is to make a systematic expansion so as to include the effect of earlier spikes

$$\begin{aligned} u_i(t) &= \eta_i^{(1)}(t-t_i^{(1)}) + \sum_{j\in\Gamma_i} w_{ij} \sum_{t_j^{(f)}\in\mathcal{F}_j} \epsilon_{ij}^{(1)}(t-t_i^{(1)}, t-t_j^{(f)}) \\ &+ \eta_i^{(2)}(t-t_i^{(1)}, t-t_i^{(2)}) + \sum_{j\in\Gamma_i} w_{ij} \sum_{t_j^{(f)}\in\mathcal{F}_j} \epsilon_{ij}^{(2)}(t-t_i^{(1)}, t-t_i^{(2)}, t-t_j^{(f)}) \\ &+ \quad \dots . \end{aligned} \tag{1.94}$$

Here $t_i^{(1)}$ is the most recent firing of neuron i, $t_i^{(2)}$ the second last firing, and so forth. If too many terms are necessary, then the approach outlined in (1.94) is not very handy. On the other hand, we may assume that the major contribution comes from the term $\eta^{(2)}, \eta^{(3)}, \dots$ and neglect the terms $\epsilon^{(2)} \dots$. Moreover, we may assume, for the sake of simplicity, that $\eta_i^{(1)} = \eta_i^{(2)} = \eta_i^{(3)}, \dots = \eta$. In fact, adaptation and even bursting can quickly be incorporated if we use a description of the form

$$u_i(t) = \sum_{t_i^{(f)}\in\mathcal{F}_i} \eta(t-t_i^{(f)}) + \sum_{j\in\Gamma_i} w_{ij} \sum_{t_j^{(f)}\in\mathcal{F}_j} \epsilon_{ij}^{(1)}(t-t_i^{(1)}, t-t_j^{(f)}) \,. \tag{1.95}$$

For the kernels η we may choose a time-course with a long-lasting contribution which could arise due to, e.g, slow calcium-dynamics [GvHC96]. An example is shown in Fig. 24. The neuron is driven with a constant input current. The $\eta(s)$-kernel has a phase of after-depolarization. As a result, a first spike at $s = 0$ makes a second spike around $s \approx 5\,\text{ms}$ more likely. A late phase of hyperpolarization in the η-kernel turns firing off after a couple of spikes. The results is, for constant input, a bursting behavior as in Fig. 24*b*.

6.3 Nonlinearities

We can distinguish at least three types on nonlinearities of neuronal dynamics. First, there is the nonlinear dynamics of spike generation. These

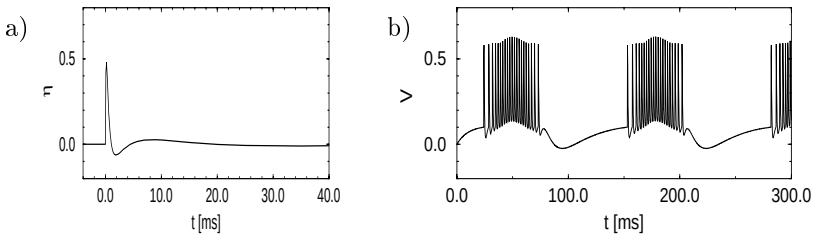

FIGURE 24. *Bursting neuron.* Constant stimulation of a neuron model with the η-kernel shown in **(a)** generates the spike train in **(b)**. Taken from [GvHC96].

nonlinearities are replaced by the output current $\gamma(s)$ which is trigerred by a threshold process as explained above. Second there are shunting effects on the dendrite due to the ion reversal potential, and finally there are potential sources of active currents on the dendrite. The last issue has been a subject of intensive discussion recently. There are indications for dendritic spikes [SS94], but it is unclear whether this is a generic feature of all neurons. In our approach, all active dendritic currents are neglected.

In the following we concentrate on the influence of the reversal potential. In sections 4 and 5 we have assumed that each input induces a standard *current* pulse $\alpha(t-t_j^{(f)})$. In more detailed models, however, the input current is due to a *conductivity* change $g(t-t_j^{(f)})$ at the synapse and the amplitude of the current depends on the present value of the membrane potential; see section 4.2. Specifically, in the context of a compartmental neuron model, the input to compartment μ is

$$I^{\mu}(t) = \sum_{j\in\Gamma^{\mu}} \sum_{t_j^{(f)}\in\mathcal{F}_j} [u_{\rm rev} - V^{\mu}(t)]\, g(t-t_j^{(f)}) \tag{1.96}$$

where $u_{\rm rev}$ is the reversal potential and $w_{ij}=1$ for the sake of simplicity.

For a further analysis of (1.96) we write $u_{\rm rev}-V^{\mu} = (u_{\rm rev}-\overline{V})-(V^{\mu}-\overline{V})$ and set $\alpha(s) = (u_{\rm rev}-\overline{V})\, g(s)$. For the potential $\overline{V}$ we take some appropriate value between the equilibrium potential V_0 and the threshold ϑ, e.g., $\overline{V} = (\vartheta - V_0)/2$. This yields

$$I^{\mu}(t) = \sum_{j\in\Gamma^{\mu}} \sum_{f} \left[\alpha(t-t_j^{(f)}) - \frac{V^{\mu}(t)-\overline{V}}{u_{\rm rev}-\overline{V}}\alpha(t-t_j^{(f)})\right]. \tag{1.97}$$

As long as $|V^{\mu}-\overline{V}| \ll |u_{\rm rev}-\overline{V}|$, the second term can be treated as a small perturbation.

Except for periods of very strong excitation or inhibition, the compartmental voltages stay roughly in the range between V_0 and ϑ. Let us look at some values. The threshold ϑ is about 10 to 30 mV above resting potential. The reversal potential of excitatory synapses is more than 50 mV above threshold. The second term in (1.97) yields therefore a small correction

only. For inhibitory synapses, the reversal potential is approximately 20 mV below resting potential, and the prefactor of the second term in (1.97) is again small. Thus we are allowed to make a perturbation expansion[2].

To proceed with the perturbation expansion, we replace V^μ on the right-hand side of (1.97) by the expression given in (1.53) and introduce $u = V^1(t)$. This yields

$$\begin{aligned} u(t) &= \sum_f \eta(t-t_i^{(f)}) + \sum_{j,f} w_{ij}\epsilon_{ij}(t-t_j^{(f)}) + \\ &+ \sum_{f,f'}\left[\sum_j w_{ij}\eta_j(t-t_j^{(f)}, t-t_i^{(f')}) + \sum_{j,k} w_{ij}w_{ik}\epsilon_{ijk}(t-t_j^{(f)}, t-t_k^{(f')})\right] \\ &+ \cdots . \end{aligned} \tag{1.98}$$

The second order kernels are for inputs $j \in \Gamma^\mu$ and $k \in \Gamma^\lambda$

$$\begin{aligned} \epsilon_{ijk}(t-t_j^{(f)}, t-t_k^{(f')}) &= \frac{1}{C^0\, C^\mu\, (E-\overline{V})} \int ds\, G^{1\mu}(s)\alpha(t-t_j^{(f)}-s) \\ &\quad \left[\int ds' G^{\mu\lambda}(s')\alpha(t-t_k^{(f')}-s-s') - \overline{V}\right] \end{aligned} \tag{1.99}$$

$$\begin{aligned} \eta_j(t-t_j^{(f)}, t-t_i^{(f')}) &= \frac{1}{C^0\, C^\mu\, (E-\overline{V})} \int ds\, G^{1\mu}(s)\alpha(t-t_j^{(f)}-s) \\ &\quad \left[\int ds' G^{\mu\lambda}(s')\gamma(t-t_i^{(f')}-s-s') - \overline{V}\right] \end{aligned} \tag{1.100}$$

Nonlinear effects at the synapses, e.g., due to calcium influx or Magnesium block removal, can be treated similarly. The role of nonlinearities for dendritic computation is discussed in [Mel94, Koc97].

6.4 Conclusions

We have presented a framework for a systematic analysis of spiking neuron models in terms of spike response kernels. As long as there are no active currents in the dendrite, the linear kernels dominate the expansion. We have demonstrated that an approach with linear response kernels is flexible and allows a phenomenological description of various types of neuron behavior including Hodgkin-Huxley dynamics. Previously, collective network states have been analyzed and stability criteria in terms of the response kernels have been derived [GvH93, Ger95, GvHC96, Cho98, Ger00]. Moreover the computational complexity of networks of spiking neurons has been analyzed in the framework of the spike response model [Maa96, Maa98]. The present

[2]For shunting inhibition, the reversal potential would be close to the resting potential and the expansion (1.98) is not helpful

paper provides a link between detailed models of neuronal dynamics and the simplified models appropriate for analytical network studies.

7 References

[Abb91] L. F. Abbott. Realistic synaptic inputs for model neural networks. *Network*, 2:245–258, 1991.

[Abe91] M. Abeles. *Corticonics*. Cambridge University Press, Cambridge, 1991.

[AFG91] L. F. Abbott, E. Fahri, and S. Gutmann. The path integral for dendritic trees. *Biol. Cybern.*, 66:49–60, 1991.

[AK90] L. F. Abbott and T. B. Kepler. Model neurons: from Hodgkin-Huxley to Hopfield. In L. Garrido, editor, *Statistical Mechanics of Neural Networks*. Springer, Berlin, 1990.

[AvV93] L. F. Abbott and C. van Vreeswijk. Asynchronous states in a network of pulse-coupled oscillators. *Phys. Rev. E*, 48:1483–1490, 1993.

[BB95] J. M. Bower and David Beeman. *The book of Genesis*. Springer, New York, 1995.

[BD91] P. C. Bush and R. J. Douglas. Synchronization of bursting action potential discharge in a model network of neocortical neurons. *Neural Computation*, 3:19–30, 1991.

[BDMK91] Ö. Bernander, R. J. Douglas, K. A. C. Martin, and C. Koch. Synaptic background activity influences spatiotemporal integration in single pyramidal cells. *Proc. Natl. Acad. Sci. USA*, 88:11569–11573, 1991.

[BH99] N. Brunel and V. Hakim. Fast global oscillations in networks of integrate-and-fire neurons with low firing rates. *Neural Computation*, 11:1621–1671, 1999.

[BT94] Paul C. Bressloff and John G. Taylor. Dynamics of compartmental model neurons. *Neural Networks*, 7:1153–1165, 1994.

[Cho98] C. C. Chow. Phase-locking in weakly heterogeneous neuronal networks. *Physica D*, 118:343–370, 1998.

[EWL+91] O. Ekeberg, P. Wallen, A. Lansner, H. Traven, L. Brodin, and S. Grillner. A computer based model for realistic simulations of neural networks. *Biol. Cybern.*, 65:81–90, 1991.

[Fit61] R. FitzHugh. Impulses and physiological states in models of nerve membrane. *Biophys. J.*, 1:445–466, 1961.

[Ger95] W. Gerstner. Time structure of the activity in neural network models. *Phys. Rev. E*, 51(1):738–758, 1995.

[Ger98] W. Gerstner. Spiking neurons. In W. Maass and C. M. Bishop, editors, *Pulsed Neural Networks*, chapter 1, pages 3–53. MIT-Press, 1998.

[Ger00] W. Gerstner. Population dynamics of spiking neurons: fast transients, asynchronous states and locking. *Neural Computation*, 12:43–89, 2000.

[GvH92] W. Gerstner and J. L. van Hemmen. Associative memory in a network of 'spiking' neurons. *Network*, 3:139–164, 1992.

[GvH93] W. Gerstner and J. L. van Hemmen. Coherence and incoherence in a globally coupled ensemble of pulse emitting units. *Phys. Rev. Lett.*, 71(3):312–315, 1993.

[GvHC96] W. Gerstner, J. L. van Hemmen, and J. D. Cowan. What matters in neuronal locking. *Neural Comput.*, 8:1689–1712, 1996.

[HH52] A. L. Hodgkin and A. F. Huxley. A quantitative description of ion currents and its applications to conduction and excitation in nerve membranes. *J. Physiol. (London)*, 117:500–544, 1952.

[JNT75] J. J. B. Jack, D. Noble, and R. W. Tsien. *Electric current flow in excitable cells.* Clarendon Press, Oxford, 1975.

[KAM92] Thomas B. Kepler, L. F. Abbott, and Eve Marder. Reduction of conductance-based neuron models. *Biol. Cybern.*, 66:381–387, 1992.

[KGvH97] W. M. Kistler, W. Gerstner, and J. Leo van Hemmen. Reduction of Hodgkin-Huxley equations to a single-variable threshold model. *Neural Comput.*, 9:1015–1045, 1997.

[Koc97] C. Koch. *Biophysics of Computation.* Oxford University Press, New York, Oxford, 1997.

[KpBD95] C. Koch, Ö. Bernander, and R.J. Douglas. Do neurons have a voltage or a current threshold for action potential initiation? *J. Comput. Neurosci.*, 2:63–82, 1995.

[Lap07] L. Lapicque. Recherches quantitatives sur l'excitation electrique des nerfs traitée comme une polarization. *J. Physiol. Pathol. Gen.*, 9:620–635, 1907. Cited in H.C. Tuckwell, *Introduction to theoretic neurobiology.* (Cambridge Univ. Press, Cambridge, 1988).

[Maa96] Wolfgang Maass. Lower bounds for the computational power of spiking neurons. *Neural Comput.*, 8:1–40, 1996.

[Maa98] W. Maass. Computing with spiking neurons. In W. Maass and C.M. Bishop, editors, *Pulsed Neural Networks*, chapter 2, pages 55–85. MIT-Press, 1998.

[Mel94] Bartlett W. Mel. Information processing in dendritic trees. *Neural Comput.*, 6(1031-1085), 1994.

[MO74] R. J. MacGregor and R. M. Oliver. A model for repetitive firing in neurons. *Kybernetik*, 16:53–64, 1974.

[MS90] R. E. Mirollo and S. H. Strogatz. Synchronization of pulse coupled biological oscillators. *SIAM J. Appl. Math.*, 50:1645–1662, 1990.

[NAY62] J. Nagumo, S. Arimoto, and S. Yoshizawa. An active pulse transmission line simulating nerve axon. *Proc. IRE*, 50:2061–2070, 1962.

[Ral64] W. Rall. Theoretical significance of dendritic trees for neuronal input–output relations. In R. F. Reiss, editor, *Neural theory and modeling*, pages 73–97, Stanford CA, 1964. Stanford University Press.

[Ral89] Wilfried Rall. Cable theory for dendritic neurons. In C. Koch and I. Segev, editors, *Methods in Neuronal Modeling*, pages 9–62, Cambridge, 1989. MIT Press.

[RE89] John Rinzel and G. Bart Ermentrout. Analysis of neural excitability and oscillations. In C. Koch and I. Segev, editors, *Methods in Neuronal Modeling*, pages 135–169, Cambridge, 1989. MIT Press.

[Rin85] John Rinzel. Excitation dynamics: insights from simplified membrane models. *Theoretical Trends in Neuroscience: Federation Proceedings*, 44(15):2944–2946, 1985.

[RL93] J. P. Rospars and Petr Lansky. Stochastic model neuron without resetting of dendritic potential: application to the olfactory system. *Biol. Cybern.*, 69:283–294, 1993.

[Rot94] Stefan Rotter. *Wechselwirkende stochastische Punktprozesse als Modell für neuronale Aktivität im Neocortex der Säugetiere*, volume 21 of *Reihe Physik*. Harri Deutsch, Frankfurt, 1994.

[RYS92] M. Rapp, Y. Yarom, and I. Segev. The impact of parallel fiber background activity pn the cable properties of cerebellar purkinje cells. *Neural Comput.*, 4:518–533, 1992.

[SNS95] D. C. Somers, S. B. Nelson, and M. Sur. An emergent model of orientation selectivity in cat visual cortical simple cells. *J. of Neuroscience*, 15:5448–5465, 1995.

[SS94] G. J. Stuart and B. Sakmann. Active propagation of somatic action potentials into neocortical pyramidal cell dendrites. *Nature*, 367:69–72, 1994.

[Ste67] R. B. Stein. The information capacity of nerve cells using a frequency code. *Biophys. J.*, 7:797–826, 1967.

[SZ98] C. F. Stevens and A. M. Zador. Novel integrate-and-fire like model of repetitive firing in cortical neurons. In *Proc. of the 5th Joint Symposium on Neural Computation*, page xx. xx, 1998.

[Tre93] A. Treves. Mean-field analysis of neuronal spike dynamics. *Network*, 4:259–284, 1993.

[Tuc88] H. C. Tuckwell. *Introduction to theoretic neurobiology*, volume 1. Cambridge Univ. Press, Cambridge, 1988.

[TWMM91] R. D. Traub, R. K. S. Wong, R. Miles, and H. Michelson. A model of a CA3 hippocampal pyramidal neuron incorporating voltage-clamp data on intrinsic conductances. *J. Neurophysiol.*, 66:635–650, 1991.

[WBUB89] M. A. Wilson, U. S. Bhalla, J. D. Uhley, and J. M. Bower. Genesis: A system for simulating neural networks. In D. Touretzky, editor, *Advances in Neural Information Processing Systems*, pages 485–492, San Mateo CA, 1989. Morgan Kaufmann Publishers.

[YKA89] W. M. Yamada, C. Koch, and P. R. Adams. Multiple channels and calcium dynamics. In C. Koch and I. Segev, editors, *Methods in neuronal modeling, from synapses to networks*, Cambridge, 1989. MIT Press.